

# Modelling spatio-temporal distribution of urban population - A high-resolution model for German cities

Peter Priesmeier<sup>a,\*</sup>, Alexander Fekete<sup>b</sup>, Michael Haberl<sup>c</sup>, Christian Geiß<sup>d,e</sup>, Roland Baumhauer<sup>f</sup>, Hannes Taubenböck<sup>e,f</sup>

<sup>a</sup> Institute for the Protection of Terrestrial Infrastructures, German Aerospace Center, Sankt-Augustin, Rathausallee 12, 53757 Sankt Augustin, Germany

<sup>b</sup> Institute of Rescue Engineering and Civil Protection, TH Köln - University of Applied Sciences, Betzdorfer Str. 2, 50679 Cologne, Germany

<sup>c</sup> Invenium Data Insights GmbH, Herrengasse 28, 8010 Graz, Austria

<sup>d</sup> Institute of Geography, University of Bonn, Bonn, Germany

<sup>e</sup> Geo-Risks and Civil Security Department, German Remote Sensing Data Center, Earth Observation Center, German Aerospace Center, Oberpfaffenhofen, 82234 Weßling, Germany

<sup>f</sup> Institute of Geography and Geology, University of Würzburg, Am Hubland, 97074 Würzburg, Germany

## ARTICLE INFO

Dataset link: [Modelling spatio-temporal distribution of urban population - A high-resolution model for German cities \(Original data\)](#)

### Keywords:

Spatio-temporal  
Population model  
Dasymetric mapping  
Urban  
Mobility

## ABSTRACT

Information about the spatial distribution of urban populations is highly relevant for areas such as urban planning, infrastructure services, and hazard prevention. Conventionally, census-based population maps provide a static image of population numbers. However, the distribution of urban populations is highly dynamic and changes throughout the course of a day, which can result in significant discrepancies from static maps. We therefore developed a spatio-temporal population model, which is designed to provide the relevant space- and time-dependent distribution for individual cities in Germany. Germany has been selected due to the high data availability, which allows us to base the model on public data, making it transferable to other cities. The city of Cologne serves as a case study, but the transfer of the approach to Hamburg has been successfully tested. The model is built on extensive dasymetric mapping cycles to combine extensive socio-demographic population and building data with mobility information. The results obtained are city-wide population maps for seven time sequences, which provide the total number of people, as well as the number of people for seven population subgroups (children, retired, etc.), on building level. The results are compared to three independent data sets (ENACT-POP, emergency call locations, and mobile phone location data), which show substantial improvement towards static census data and good correlation metrics. The spatio-temporal results show strong time-dependent differences in comparison to static population distribution (e.g., up to six times more people for the inner city of Cologne at midday), underlining the relevance of time-dependent data for population-based analyses.

## 1. Introduction

By 2050, 68% of the world's population will live in cities (UNDESA, 2019). With it, humankind will face growing challenges to ensure sustainable development, efficient provision of critical services, and the protection of its citizens, among other issues. Thus, it is essential for the relevant domains, such as urban planning, traffic management, critical infrastructure development, or disaster management, to understand, among other variables, the spatial distribution of the citizens within the urban boundaries. Traditional population mapping assigns statistical

census data or, more recently, remotely sensed information to administrative spatial units (Geiß et al., 2022; Geiß et al., 2024; Leyk et al., 2019; Sapena et al., 2022; Taubenböck et al., 2007). Such datasets typically offer only a static snapshot of the population's distribution. Depending on the method, they often depict the nighttime situation, where most people are located at their place of residence. Such static population data stands in direct contrast to the high mobility that the population actually exhibits over the course of the day (Ahola et al., 2007; Batista E Silva et al., 2020; Deville et al., 2014; Doyle et al., 2014; Freire et al., 2013; Gariazzo et al., 2016; Martin et al., 2015; Pittore

\* Corresponding author at: Deutsches Zentrum für Luft- und Raumfahrt (DLR), Institut für den Schutz terrestrischer Infrastrukturen, Rathausallee 1253757 Sankt Augustin, Germany.

E-mail addresses: [peter.priesmeier@dlr.de](mailto:peter.priesmeier@dlr.de) (P. Priesmeier), [alexander.fekete@th-koeln.de](mailto:alexander.fekete@th-koeln.de) (A. Fekete), [Michael.haberl@invenium.io](mailto:Michael.haberl@invenium.io) (M. Haberl), [cgeiss@uni-bonn.de](mailto:cgeiss@uni-bonn.de) (C. Geiß), [roland.baumhauer@uni-wuerzburg.de](mailto:roland.baumhauer@uni-wuerzburg.de) (R. Baumhauer), [hannes.taubenboeck@dlr.de](mailto:hannes.taubenboeck@dlr.de) (H. Taubenböck).

<https://doi.org/10.1016/j.compenvurbsys.2026.102419>

Received 28 October 2025; Received in revised form 30 January 2026; Accepted 18 February 2026

Available online 9 March 2026

0198-9715/© 2026 The Authors. Published by Elsevier Ltd. This is an open access article under the CC BY license (<http://creativecommons.org/licenses/by/4.0/>).

et al., 2023; Renner et al., 2018; Yoongsomporn et al., 2025). While a residential area can be densely populated during the night, its residents might move to business districts, university campuses, or the local inner-city shopping mall during the day. A single, static population map of a city cannot consider these daily population dynamics, which makes analyses and decisions based on such data prone to severe misestimations.

In complex urban environments, a variety of fields would profit from dynamic population data, especially if it is nationwide and publicly available. Urban planning can be enhanced by providing services not only based on citizens' residence locations, but also on where people are actually located during the day. Traffic modelling and public transport demand analyses also need to understand daily population mobility. Critical infrastructure providers for services like water or electricity could enhance their daytime-dependent demand analyses. Especially Disaster management would seem to profit from dynamic population data, due to a high number of use cases. Dynamic population data could be used to improve the planning for new fire and rescue station locations and their necessary capacities. Risk analyses, especially for sudden onset disasters, need to take the time-dependent location of citizens into account if they want to predict reliable numbers of affected. If dynamic population data includes information about socio-economic subgroups, those could be used to cover the demand for dynamic vulnerability analyses (Aubrecht, 2013a; Cutter et al., 2000; Haraguchi et al., 2022). The previous examples underline the manifold demand for publicly accessible spatio-temporal population data (Aubrecht, 2013b; Behrens et al., 2021; Cui et al., 2021; Pittore et al., 2017).

Even though Germany offers a multitude of population-related datasets, with many of them being publicly available or at least free of charge for research purposes, there is, up till now, to our knowledge, no high-resolution spatio-temporal population dataset available. We therefore develop a spatio-temporal population model that focuses on German cities and estimates the number of people present in individual buildings at seven different time intervals of the day. A key constraint of the model is the restriction to the usage of publicly accessible data. This secures the transferability to other German cities and provides an alternative to approaches focused on single cities or expensive data (e.g., from mobile phone companies). With a focus on public data and our high spatial and temporal resolution, we aim to offer an easily accessible solution to close the gap in spatio-temporal population data for German cities.

### 1.1. Research context

Generating results that adequately represent daily population behavior demands either highly detailed geospatial data and mobility information or extensive amounts of human positioning data. We divide the currently existing approaches for spatio-temporal population models into two types, depending on the data they use. 1) The positioning data-based approaches use measurements directly retrieved from real-world human mobility data (e.g., mobile phone logins to cell towers, GPS signals) and extrapolate insights to the whole investigated population. 2) The dasymetric mapping approach combines geodata with static demographic data about the area's population and models their mobility indirectly based on mobility information (e.g., surveys). In the following paragraphs, we briefly discuss both approaches and explain why our model uses the dasymetric approach. Afterwards, an overview of previous dasymetric approaches is provided. In doing so, we focus on data sets with intra-day population changes. Renowned data sets such as WorldPop (Tatem, 2017), Global Human Settlement Layer (Pesaresi et al., 2024) or LandScan Global (Lebakula et al., 2025), which calculate high-resolution global population data but are only available on an annual basis at most, are not taken into account.

#### 1.1.1. Real-world positioning data

The application of direct measurements from real-world positioning data has grown more common in recent years (Yabe et al., 2022).

Mobile phone data, mostly the log-on of phones to radio towers (Bengtsson et al., 2011; Chen et al., 2020; Deville et al., 2014; Doyle et al., 2014; Haberl et al., 2025; Han et al., 2019; Liu et al., 2018; Yoongsomporn et al., 2025) or GPS positions (Rahimi-Golkhandan et al., 2021; Wang et al., 2020; Wang & Taylor, 2018; Yabe et al., 2020) is commonly used to generate spatio-temporal population maps. Other sources, like smart cards (Zhao et al., 2017; Zhong et al., 2016) or public transport transactions (Zhao et al., 2017; Zhong et al., 2016) as well as bus and taxi GPS data (Zhang et al., 2019) have potential, but are more often employed to understand mobility patterns instead of calculating spatio-temporal population maps (Cats, 2024).

The advantage of such real-world positioning data is the in situ knowledge on positioning at a particular time and the retention of mobility information. While geostatistical, dasymetric approaches have to estimate the population's location and mobility, positioning data is based on real localisations of people. The disadvantages are that the spatial resolution can be tied to metrics like the density of the radio tower network and that such data only depicts the population with smartphones (Pappalardo et al., 2023; Wardle et al., 2023). In consequence, vulnerable groups, like young children and the elderly are underrepresented in such data and thus can be underestimated (Sekara et al., 2019) which constrains its use in fields like disaster management. In addition, datasets usually only cover a portion of the total population, depending on how large the market share of the company from which the data originates is, making extrapolations necessary. In Germany, Vodafone holds the biggest share with 42,8% in 2023 (Tenzer, 2024). Lastly, the dependence on private companies to obtain data and the respective high cost limit its applicability in research, especially if the application is planned to go beyond a single case study.

#### 1.1.2. Dasymetric approaches

Dasymetric approaches, on the other hand, build on heterogeneous but static data by combining geodata, census statistics, and mobility information to distribute population spatially and temporally (Batista E Silva et al., 2020; Martin et al., 2015; Renner et al., 2018). One disadvantage is the demand for extensive, high-resolution geodata about citizens and activity locations, as well as detailed mobility behavior information. However, due to the global increase in data generation and its public availability, data fulfilling the necessary requirements for population modelling and the respective validation are now available for more and more regions. Dasymetric methods, therefore, start to provide a competitive alternative to the usually expensive position data-based approaches.

Germany provides such a necessary data landscape, where detailed census data (City of Cologne, 2024c) as well as geodata, including the size and usage type of buildings (Cologne District Government, 2025), are available publicly or by request throughout all major German cities. The regularly conducted mobility survey "Mobilität in Deutschland" (MiD) (Nobis & Kuhnimhof, 2018) provides extensive mobility information. This presents the ideal basis for a model that is transferable to several German cities based solely on cost-free data. We therefore opt for the dasymetric approach and introduce a spatio-temporal population model variant that provides population counts for different population subgroups on building level for several time intervals of a standard working day.

Our approach builds on extensive previous work starting with Ahola et al. (2007) and Taubenböck et al. (2007). The first study set a foundation with a spatio-temporal population disaggregation based on building types and up to six time intervals per day for a bomb blast exposure scenario. The second one used a day- and nighttime perspective for an earthquake scenario. Building upon their work in Freire

(2010) and Aubrecht (2013b), both authors developed a spatio-temporal population exposure model for earthquakes (Freire & Aubrecht, 2012), which is improved by an evacuation component by Freire et al. (2013). They use land cover classes and road types to define residential and labor areas on which census data is disaggregated into a day- and a night-time map. In combination with hazard maps and with a walking time-based evacuation model, it becomes apparent that the amount of exposed population in the case study of Lisbon has been underestimated by far. Aubrecht et al. (2014) further developed the DynaPop-X Model, which adds commuters to the previous approach. With it, they aim towards higher temporal resolution, and the model is applied to a storm surge scenario (Aubrecht et al., 2015). Taubenböck et al. (2013) focus on tsunamis and identify daytime-dependent degrees of exposure and bottlenecks in the traffic system in Padang, Indonesia, for evacuation measures. Martin et al. (2009, 2015) developed the Population 24/7 model, a flexible and transferable model framework that is adjustable to different data scenarios. In their use case for the city of Southampton, they implement census data and capacities of destination points like schools, universities, or hospitals, and roads. The method assigns a time-dependent population capacity and a supply area to origin and destination points, as well as the connecting road network. A 200 m raster grid weight map is calculated from this information, which is used to assign residential population to grid cells per 15-min time interval, based on estimated distance bands. The approach is updated with time graphs, more destination assets, and information about the non-residential population by Smith et al. (2016), who apply the results in a flood exposure analysis. Renner et al. (2018) transfer the model to the Autonomous Province of Bolzano, where they investigate the daily and seasonal changes of population exposure in hazard-prone areas. The Population 24/7 model is available for the UK and is based on the 2011 census (Cockings et al., 2021). Pittore et al. (2023) model day- and night-time as well as commuting population based on high-resolution commuter and population data with hexagons as spatial units. The results are used to analyze multi-hazard exposure and disaster-induced traffic changes. Rauch et al. (2021) calculate the day and night population for the government district of Münster to investigate the time-dependent coverage by the rescue service, and are thereby to our knowledge, the only comparable German case study. A Europe-wide approach, and therefore to our knowledge the only spatio-temporal dataset, that is also available for entire Germany is the ENACT-POP dataset (Schiavina et al., 2020). It offers a 1 km grid with estimated population distribution in day- and night-time per month for all EU countries, based on official statistical data for the census year of 2011 (Batista E Silva et al., 2020). LandscanHD, developed by the Oak Ridge National Laboratory (ORNL) (Tuccillo et al., 2025), is a day and night population dataset aiming for global coverage. The product is based on a global dataset of building footprints, usage types, and heights, created by combining globally available products with a variety of self-developed methods. Country-specific facility occupancy rates (Urban et al., 2023) are used to disaggregate national population data to a one-arc-second grid. While data for various countries is available to date, unfortunately, no results have been published for Germany yet.

### 1.2. Aims and research questions

We identified a lack of spatio-temporal population data with high resolution, be it on the spatial, temporal, or semantic level, while at the same time, recognizing the great potential to improve existing applications of dynamic intra-day population data (e.g., disaster management, traffic and infrastructure demand modelling, urban planning). While not every region is (yet) able to meet the high associated data requirements, it looks like more and more countries are on a good way to provide a data landscape that is able to satisfy these demands.

We aim to utilize the meanwhile extensive data availability in Germany to design a model that provides population maps with a high spatio-temporal resolution in major cities, free of charge, and accurate

enough to be useful for a wide range of applications. To meet this demand and to advance the state of research, we define the following requirements, followed by respective research questions.

To ensure transferability, our model will only use data that is available throughout Germany. Germany's sixteen federal states have different open data policies; therefore, we do not demand data to be publicly available in all states, but it has to be at least available on request. In terms of temporal resolution, we aim beyond a pure day and night division towards several time intervals per day. The spatial resolution aims to reach sufficient accuracy on building level, so that the results can be used for varying spatial units (e.g., flood masks) while limiting the modifiable aerial unit problem (Openshaw, 1984). To enable deeper population analyses (e.g., social vulnerability), the model needs to consider not only the population, but also model its subgroups separately (e.g., children, elderly). Altogether, the necessary computing power is to remain reasonable, so that the transferability is not limited by the need for high computing capacities.

The model results will subsequently be used to investigate the following research questions:

- What novel insights about the time-dependent urban population can be gained from the model compared to the statistical data previously available? How big is the difference?
- How accurate is the model and what uncertainties is it subject to? What are the resulting implications for the use of the data?
- Is the data publicly available in Germany sufficient enough to gain satisfactory results with dasymetric spatio-temporal population modelling approaches

## 2. Model

The model's framework is structured into four steps (Fig. 1).

Step ① divides the data preprocessing into three sub-steps. First, activity profiles for seven population subgroups (e.g., Children, Fulltime Workers) are designed, based on an extensive mobility study. Afterwards, the population of the area investigated is grouped into these subgroups, based on socio-demographic geodata. Finally, all buildings of the study area are assigned to one of 50 building types, based on size, usage type, and expected population density.

Step ② uses the refined population data and building information to generate a base residence map that calculates how many people of each group live in each building. It also serves as the starting point for modelling.

Step ③ divides the time-dependent assignment of population to buildings into three sub-steps. First, the base residence map is divided into hexagonal calculation units to reduce calculation time. All underlying information is aggregated from building to hexagon level. This is followed by a looped mobility modelling approach that moves fine-grained population shares of each subgroup between the hexagons based on daytime, travel distance, as well as number and type of conducted activities. Afterwards, the new population counts per hexagon are disaggregated back down to building level.

Step ④ includes commuters coming from outside the city area.

The model is programmed with R Studio on R 4.5.1 as a case study independent code framework, which is transferable to major German cities.

### 2.1. Step ①: data preprocessing

The city of Cologne, Germany, serves as a case study and testing ground for the model development. A strong focus is kept on maintaining the transferability to other cities. We therefore limit the data needed for our approach to basic datasets available to all German authorities according to Germany's National Geoinformation Strategy 2.0 (GDI-DE, 2025). This also means that the used data follows the EU INSPIRE Directive (European Commission, 2025), which simplifies a

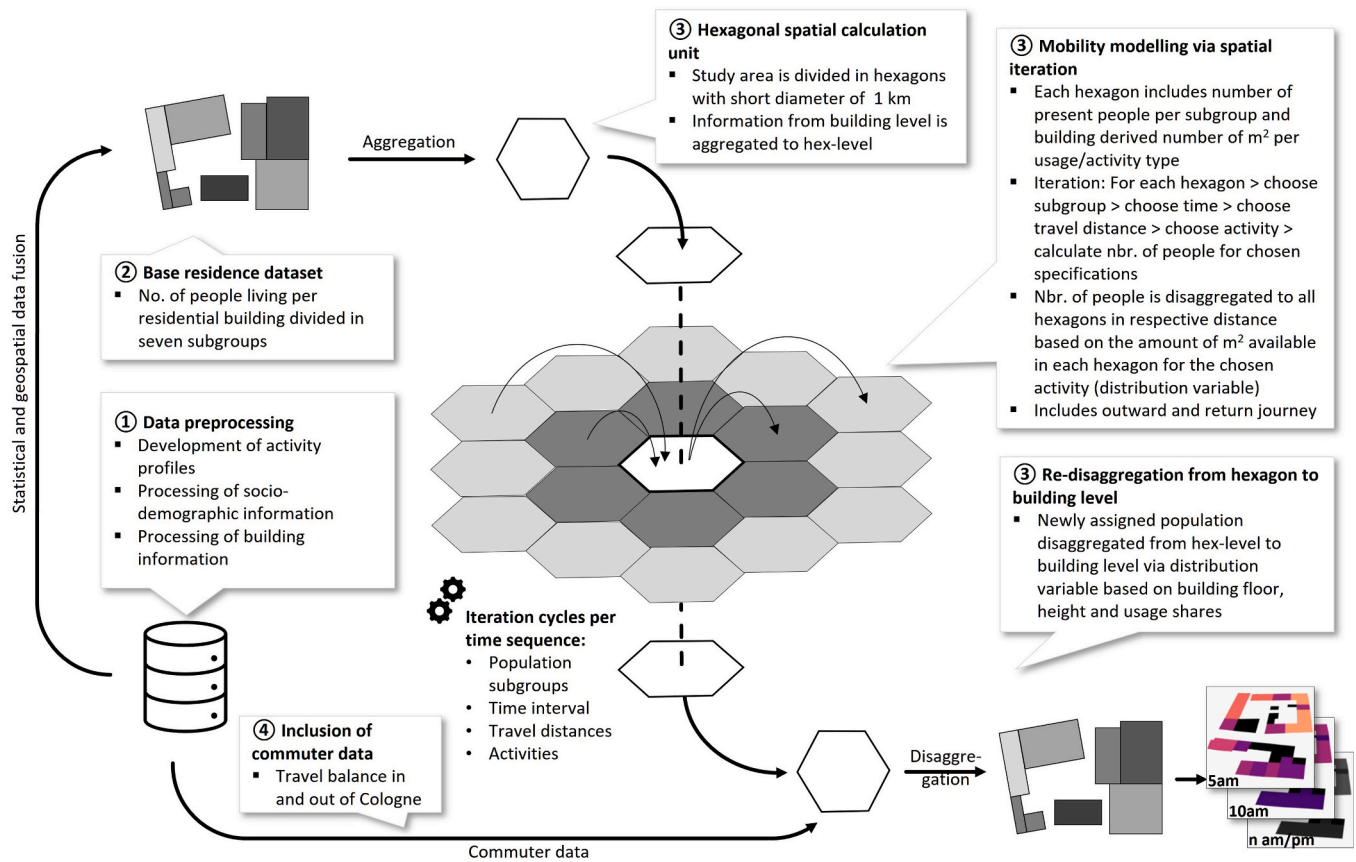


Fig. 1. Framework of the spatio-temporal population model. The numbers link to the following chapters.

possible future transfer of the approach to cities outside of Germany. It has to be noted that the data is not available publicly for every city, due to different data policies in Germanies 16 federal states, but it is available and can be requested via the responsible authorities.

### 2.1.1. Development of activity profiles

Activity profiles summarize the daily behavior of urban populations and thus allow population groups to be assigned to specific mobility patterns. Information about the mobility behavior of Germany's population stems from the "Mobilität in Deutschland (MiD)" study (Follmer, 2025) with over 420,000 participants. It includes a detailed multi-step procedure where participants monitor their mobility behavior on a randomly assigned day (Follmer, 2025). Considerable effort was made to minimize potential bias and ensure that the results were representative. Various collection methods (online, telephone, postal) were used, missing values were imputed, and the data were comprehensively weighted to compensate for deviations between the extensive sample and the actual population structure. Our approach is based on these latest and corrected results from 2023, which allow us to create detailed activity profiles for population subgroups as well as distance patterns for trips to daily activities.

The study provides the total number of trips taken for seven subgroups (children, pupils, students, fulltime workers, parttime workers, jobless, and retired). All trips are divided by the activity the trip is taken to and by the travel distance (0–0.5 km, 1 km, 2 km, 5 km, 10 km, 20 km, 50 km, 100 km and above) and the arrival time interval (5 am – 8 am, 10 am, 1 pm, 4 pm, 7 pm, 10 pm, 5 am). It further provides side information, like the share of a subgroup that takes a certain number of trips per day. The latter allows us to include the amount of activity specifically for each subgroup, by calculating the percentage of people staying at home (no activity) or pursuing one or two activities per day. In terms of the activities themselves, we distinguish between four main and six

**Table 1**  
Possible activities per activity profile.

Population subgroup	Main activity	Secondary activity
Children	Daycare	Shopping, private errands, visiting friends, leisure-general, leisure-sport and leisure-going out
Pupils	School	
Students	University	
Fulltime workers	Work	
Parttime workers	Work	
Jobless	Shopping, private errands, visiting friends, leisure-general, leisure-sport, and leisure-going out	
Retired		

secondary activities (Table 1). Being at daycare, school, university, or work are the main activities that children, pupils, students, or full- and parttime workers pursue on a standard working day, if they do not stay at home. Secondary activities are shopping, private errands, visiting friends, leisure-general, leisure-sport, and leisure-going out, which are conducted as the second activity during a day. For the activity profiles of jobless and retired, the main activities are the same as the secondary activities (Table 1). This allows us to determine which share of a subgroup stays at home or pursues a main activity or a main activity followed by one or more secondary activities for a standard working day (Tables A1–A7).

We use the distribution of trips by time, which is available in the survey for each subgroup, to break down the previously calculated shares. For this, we calculate at what time which share of a subgroup arrives at an activity. The MiD study also provides numbers on trips taken to go home, which we use to calculate the share of people leaving

their main activity to go back to their residence. For the six secondary activities, like shopping or private errands, we combine information from 30 sub-activities. These secondary activities are usually shorter than the time intervals of two to three hours in our model. Thus, we assume that people arriving at a secondary activity also leave again during the same time interval. The whole process enables us to calculate which percentage of a subgroup pursues which activity at what time of day, resulting in activity profiles providing the percentage of people that are “at home”, “arrive to” or “leave from” a certain activity per time interval (Tables A8–A14). Table 2 provides a summary of the activity profile for the subgroup “Fulltime Worker”, where the secondary activities have been combined for better visualization. Fig. 2 displays the percentage of people pursuing main and secondary activities throughout the day. These relative activity profiles build the foundation for the fine-grained population distribution in the next steps.

After integrating the number of daily activities and the temporal component, we add the spatial component, through which we assign the previously calculated subgroup shares to specific locations. The MiD study allows us to determine the distance people travel to a specific activity at certain times. This is later used to narrow down the buildings people travel to. This information is combined into time-dependent distance profiles for each activity (Table 3). We only use distances up to 50 km, since distances up to 100 km and more only make up 3% of all trips and would result in quadruple calculation time. Since the model calculates distances in a straight line, but the MiD values come as the actual road-bound travel distance, we reduce the distances by 28%. This value was derived manually by plotting isochrones for all distances from the center of Cologne city based on the local road network and measuring the distances from the center to ten random points on each isochrone's edge. On average, the traveled distance via road was 28% less than the straight line (Table 3). We further combine the distances 0.5 km and 1 km since both are smaller than our later implemented hexagonal spatial calculation units with 1 km diameter (2.3. Step ③: Spatio-temporal population distribution). The distance profiles are later used to define where people move from their homes for certain activities. The activity profiles thus contain the information for each subgroup as to which proportion of these people pursue which activity at which time of day, and where (in relation to their starting point) they travel to do so (Tables A15–A19).

**Table 2**  
Extract of the “Fulltime Worker” activity profile.

Fulltime worker					
Time interval	Being at home	Main activity “work”		Summary of all secondary activities	
		Arrival at work	Leave work	Arrival at second	Leave secondary
5 am–8 am	46.61%	+51.30%	−1.80%	+2.09%	−1.27%
8 am–10 am	23.05%	+22.50%	−3.60%	+6.75%	−2.09%
10 am–1 pm	17.27%	+5.40%	−8.10%	+15.23%	−6.75%
1 pm–4 pm	29.34%	+5.40%	−17.10%	+14.86%	−15.23%
4 pm–7 pm	55.64%	+1.80%	−36.00%	+22.76%	−14.86%
7 pm–10 pm	84.66%	+1.80%	−17.10%	+9.04%	−22.76%
10 pm–5 am	96.93%	+1.80%	−6.30%	+1.27%	−9.04%
Sum times		*+90.00%	*−90.00%	*+72.00%	*−72.00%

\* 10% of the “Fulltime Workers” stay at home, e.g., due to vacation or illness; 72% conduct a secondary activity on top of their main activity.

### 2.1.2. Socio-demographic information

Socio-demographic information is used to group the city's population into the seven subgroups. For Cologne, the “Statistical Data Catalogue Cologne” (SDC) (City of Cologne, 2024c) provides detailed socio-demographic information like age composition, number of pupils, or number of socially insured workers at the level of the 570 districts. One district is a sub-district unit and encloses the area of 1000 to 3000 people with a homogenous demographic structure (City of Cologne, 2024c). We calculate the number of people per subgroup on the district level by combining the SDC and general German statistical information (Table 4). All people till the age of six are assigned to the subgroup of children. The number of pupils per district is directly available in the SDC. For the students, we take 26% of the 18–24 age group, which is the average share of students according to the Federal Statistical Office of Germany (2024). For 2023, this method leads to an overestimation of 1.8% of the actual student numbers for Cologne (City of Cologne, 2024a). The number of fulltime workers is calculated by the number of socially insured workers (City of Cologne, 2024b) with an addition of 25%, which represents the privately insured workers (City of Cologne, 2018). These values are difficult to verify, since the latest statistics for the privately insured workers date back to 2016. In comparison with a number extrapolated from unemployment statistics, we reach 92% of the total workers living in Cologne (Federal Employment Agency of Germany, 2024). Parttime workers account for 25% (City of Cologne, 2024a) of the socially insured workers, but since these number includes the 63% of the students, who work while studying (Kroher et al., 2023), they are subtracted to not be counted twice. The jobless subgroup consists of unemployed people who are recorded in the statistics of the labor agency, plus people who are not working but do not appear in the unemployment statistics (e.g., houseman/woman), which we calculate with 2.5% of the total population (Wipperman, 2016). To calculate the number of retired people per district, we use the number of people older than 64, from which 9%, who are still working, according to the Federal Statistical Office of Germany (2023), are deducted.

### 2.1.3. Building information

Buildings are the spatial foundation of the model and function as dispensing, receiving, and collecting units for the mobile population. They are assigned activity-dependent building types and weightings in order to facilitate this distribution. To estimate the residential population as well as the day-time dependent inflow and outflow of each building, information such as usage type, floor area, and number of floors is required. We use information from the “Amtliches Liegenschaftskatasterinformationssystem (ALKIS)” (Official property cadaster information system) (Cologne District Government, 2025), which includes all buildings in Germany and is either available publicly or upon request. ALKIS provides the footprint and floor number for every building and assigns it to one of 235 usage categories, which include a standardized name and a description of what the building is used for. We use this to filter out buildings below 25 m<sup>2</sup> and irrelevant categories like stairs or garages.

The number of people that will be assigned to a building depends on the size of the building and on its type of use. We differentiate this via 50 building activity types, which are developed in three steps. First, we group the ALKIS building categories into twelve building activities (Table 5) that match the previously developed activity profiles (e.g., Work, Residential). Secondly, we assign density weights based on the number of people expected in a building, since buildings might be occupied by a different number of people, even if they have the same activity type assigned. As an example, for the activity “work”, an office building has a higher density of workers per square meter than a factory building or a power plant. This occupation density weight allows us to create building types that differentiate between population density in buildings within the same building activity (e.g., Work25, Work100, Residential30, Residential60). The height of the weights themselves is based on the description of the 235 building categories from the ALKIS

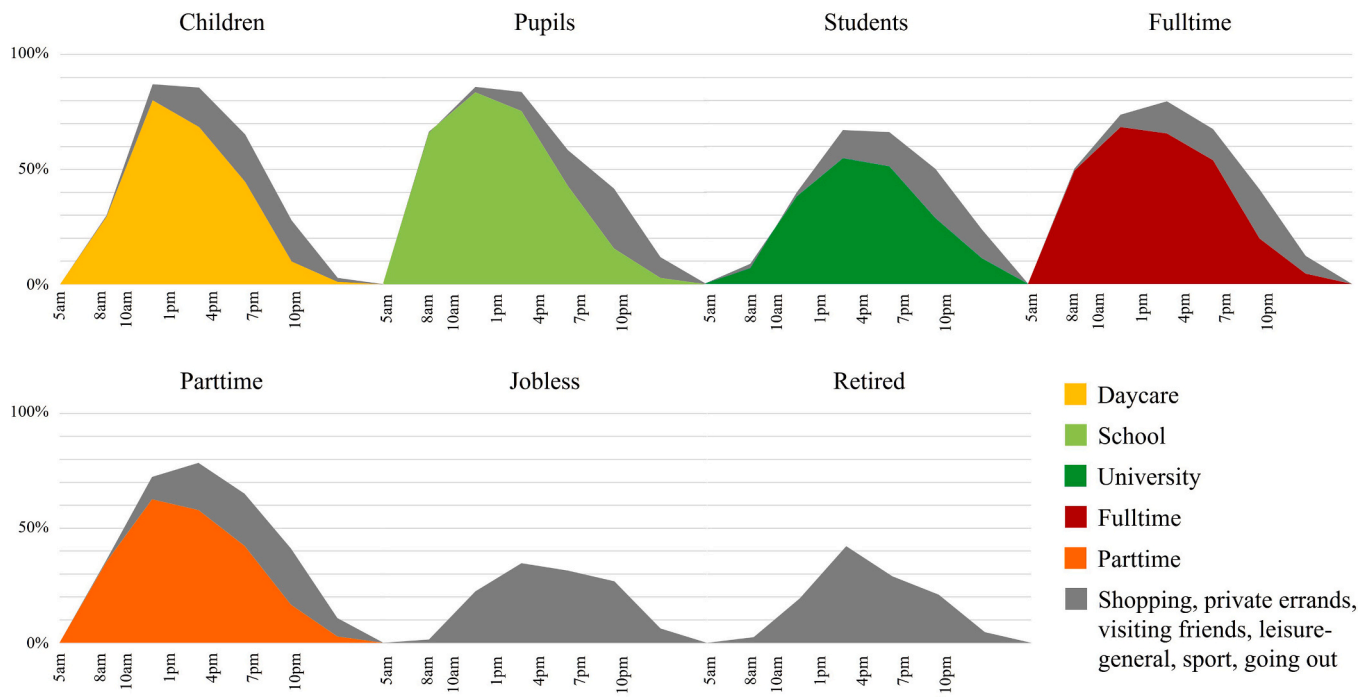


Fig. 2. Share of people attending a certain activity during a standard working day per subgroup.

**Table 3**  
Distance profile for the activity “Work”.

Time	Distances*						Sum
	0.36 km	1.44 km	3.6 km	7.2 km	14.4 km	>36 km	
5 am–8 am	7%	7%	19%	21%	25%	21%	100%
8 am–10 am	8%	9%	20%	21%	22%	20%	100%
10 am–1 pm	18%	11%	23%	18%	17%	13%	100%
1 pm–4 pm	21%	12%	23%	19%	15%	10%	100%
4 pm–7 pm	19%	13%	21%	19%	17%	11%	100%
7 pm–10 pm	10%	8%	22%	19%	22%	19%	100%
10 pm–5 am	9%	9%	19%	20%	26%	17%	100%

\* Original distances reduced by 28% to convert them from road-bound travel distances to straight-line distances.

**Table 4**  
Conversion of socio-demographic data from the city of Cologne to the model subgroups based on the MiD study.

Subgroup	Calculation
Children	Number of 0 to 6-year-olds
Pupils	Number of pupils by place of residence * 0.645
Students	Number of 18–24 years old * 0.26
Fulltime	Number of socially insured workers * 1.25 - socially insured workers * 0.25
Parttime	Number of socially insured workers * 0.25 - number of students * 0.63
Jobless	Number of unemployed + 0.025 * total number of people
Retired	Number of over 64 years old * 0.91%

dataset. In unclear cases, aerial imagery from Google Maps is used to gain a better understanding of the buildings belonging to the respective type. In the third step, we develop dual activity types, since most buildings are used for more than one activity. E.g., residential buildings

**Table 5**  
Building activity types, which are used to generate building type combinations.

Building activity	Description	Examples building categories
Residential/At home	Places where people live	Residential house, apartment building
Daycare	Kindergarten or pre-school daycare	Kindergarten, daycare center
School	All types of schools, 1st – 13th grade	Elementary School, vocational school
University	Public and private Universities	University, college, private universities
Work	Places where people work	Office building, factory
Shopping	Supermarkets and other shops	Supermarket, shoe shop, clothing Store
Private errands	Places for private errands	Doctor, insurance, post, hospital
Leisure-general	Places to carry out hobbies and cultural activities (not sports)	Theatre, opera, museum, amusement park
Leisure-going out	Places for going out or eating	Bar, restaurant, casino
Leisure-sports	Places for sports	Gym, Swimming pool, soccer field
Leisure-visiting friends	No own designated building type, instead residential is used	Residential house, apartment building
Empty	Places that are mostly unoccupied during a standard workday	Car park, reactor building, church, transformer station, Stable

with a store on the first floor or elderly homes, where people live and work at the same time. For ALKIS categories that suggest double use, existing building activities are combined (e.g., Residential30\_Work100, Work87.5\_Private25). It is important to note that the weights only count within the same activity (e.g., Work) and not across activities. This approach results in 50 different building activity types that cover the 235 building categories from ALKIS (Table A20).

For the activity of “shopping”, the locations of supermarkets and shops are needed. ALKIS does not provide this information for dual activity buildings, so we use points of interest from Open Street Map

(OSM) (OpenStreetMap Contributors, 2025) instead. The OSM locations of supermarkets and shops are used to assign shopping weights to respective buildings. Since OSM data is not always reliable, only buildings with an ALKIS building category that matches commercial use are updated. A similar problem exists with day-care centers for children. Here, we use a list of day-care centers from the City of Cologne (City of Cologne, 2022), which are geocoded via their addresses in ArcGIS Pro. The locations are assigned to the closest matching building type, which is then upgraded with a daycare share.

The final building dataset (Tables 6 and 7) provides for each building the height and footprint-based usage area, as well as the building type consisting of up to two different usage types, which are weighted according to the number of people expected to pursue the respective activity. This allows us to calculate distribution variables (building area \* number of floors \* activity weight; detailed version in Appendix B), which function as elaborated weights to later assign the right share of people to the right buildings (Table 7).

## 2.2. Step ②: base residence dataset

The base residence dataset serves as the starting point for the population modelling. It shows the number of people of each subgroup living in the city's residential buildings. For this purpose, the subgroup counts at the district level are dasymmetrically disaggregated to buildings with a residential share, by setting the residential distribution variable (building area \* floor number \* residential weight) per building in relation to the variable's sum per district. This allows a detailed allocation of the subgroups throughout the whole city based on the underlying socio-demographic structures and urban fabric.

## 2.3. Step ③: spatio-temporal population distribution

In order to map the time-dependent location of citizens, the model calculates which people pursue which activities at what place and at what time. For this purpose, we implement a hexagon tessellation of the city area to distribute the population between hexagons based on their activity profile (Table 1), the activity-associated time intervals (Table 2), the distance profiles (Table 3), and the building information (Tables 6 and 7).

### 2.3.1. Hexagon tessellation and data aggregation

Hexagons are used as spatial data containers that aggregate the data

**Table 6**  
Extract from the final building dataset attribute table.

No.	Story	Base area	Usage area	ALKIS category (translated)	Type
1	12	350 m <sup>2</sup>	4200 m <sup>2</sup>	Office building	Work100
2	1	61 m <sup>2</sup>	61 m <sup>2</sup>	Refugee center	Residential100
3	2	109 m <sup>2</sup>	218 m <sup>2</sup>	Residential building	Residential70
4	4	101 m <sup>2</sup>	404 m <sup>2</sup>	Residential building with commerce and services	(updated via OSM POIs) Residential50_Shopping25
5	4	91 m <sup>2</sup>	364 m <sup>2</sup>	Residential building with commerce and services	Residential50_Work25
6	3	1179 m <sup>2</sup>	3537 m <sup>2</sup>	Museum	LeisureGeneral100
7	5	438 m <sup>2</sup>	2190 m <sup>2</sup>	Insurance	Work90_Private25
8	4	4927 m <sup>2</sup>	19,708 m <sup>2</sup>	Hospital	Work50_Private50

of the underlying buildings. This intermediate step is necessary, since modelling the population movement between single houses would result in an unfeasible calculation effort (The city of Cologne alone consists of over 225,000 buildings). The hexagons were created with a short diameter of 1 km (0.87 km<sup>2</sup>) using the tool "Generate Tessellation" in ArcGIS Pro 3.6.1. The size is adjustable, but 1 km provides a good tradeoff between accuracy and calculation time. Test runs with 1.5 km (1.95 km<sup>2</sup>) and 0.75 km (0.49 km<sup>2</sup>) hexagons, lead to half, respectively, five times the computation time of 2 h necessary for the 1 km run. In comparison with the mobile phone location data, which we use as a ground truth validation dataset in chapter 3.2.4. Comparison of results with mobile phone location data", 1.5 km hexagons lead to a mean absolute percentage error (MAPE) increase of 2%, while 0.75 km hexagons lead to a MAPE decrease of 1%. Compared on building level, the 0.75 km version results in 5,5%, the 1.5 km version in 5,7% MAPE per building through all time intervals.

We choose hexagons since they form near circular patterns and provide a more even and symmetric base for measuring distances in a circular way, and minimize ambiguity in defining the nearest next units from a center point, compared to common square grids (Birch et al., 2007; Pittore et al., 2023). All underlying building and population information (e.g., sum of people per subgroup living in a hexagon, sum of distribution variables per building activity type) is aggregated to hexagon level (Fig. 3). This reaggregation from districts to buildings to hexagons ensures that the underlying socio-demographic and urban fabric is preserved and that the later re-disaggregation to building level stays feasible.

### 2.3.2. Activity informed population distribution

Once all building and population information from the base residence dataset is aggregated to hexagon level, the model calculates for each hexagon the outgoing population, their respective target hexagon, and the population flowing into the hexagon from other hexagons. The formulas for this process are available in Appendix B. In detail, this process works as follows, exemplified in one repetition cycle for one hexagon: First, a subgroup, a time interval, a distance, and a main or secondary activity are selected. The aggregated values from the base residence dataset now allow us to calculate the number of people who leave (or come back to) the hexagon for the defined combination of time, activity, and travel distance. The travel distance is then used to identify possible target hexagons, which are located in the right range. Then, the people are assigned to these hexagons based on their share of buildings fitting for the selected activity (via the previously calculated distribution variable derived from building activity type, area, floor number, and weight).

For the exemplary hexagon depicted in Fig. 4, we can identify 260 fulltime-workers (subgroup), who leave work (main activity) between 1 and 4 pm (time interval) and have a straight-line travel distance to their homes between 1.44 km to 3.6 km (distance). The 260 workers are now divided between all hexagons in the respective distance from the starting hexagon, while hexagons with more residential living space get more people assigned. The amount of living space is based on the sum of the residential distribution variables of all buildings in the respective hexagon.

The process described is repeated for all hexagons, for the seven subgroups and with their main and secondary activity, the seven time intervals, and the seven distances, resulting in ca. 1.18 million calculation steps. This allows for a precise distribution of small groups of people between hexagons, which have the same daily behavior. The results cover an area of 36 km around Cologne. For each hexagon, the sent and the received number of people are recorded per subgroup, activity, time interval, and distance. The numbers collected are consecutively disaggregated back to building level based on the distribution variables and (dual) building types. This ensures that large buildings with high activity weighting and therefore high distribution variable values get more people allocated and removed than smaller

**Table 7**  
Continuation of the previous extract from the final building dataset attribute table.

No.	Usage area	Type	Residential weight	Work weight	Resid. distribution variable	Work distribution variable
1	4200 m <sup>2</sup>	Work100	0	1.0	0	4200
2	61 m <sup>2</sup>	Residential100	1.0	0	61	0
3	218 m <sup>2</sup>	Residential70	0.7	0	152,6	0
4	404 m <sup>2</sup>	Residential50_Shopping25	0.5	0	202	0
5	364 m <sup>2</sup>	Residential50_Work25	0.5	0.25	182	91
6	3537 m <sup>2</sup>	Leisure General100	0	0	0	0
7	2190 m <sup>2</sup>	Work90_Private25	0	0.9	0	1971
8	19,708m <sup>2</sup>	Work50_Private50	0	0.5	0	9854

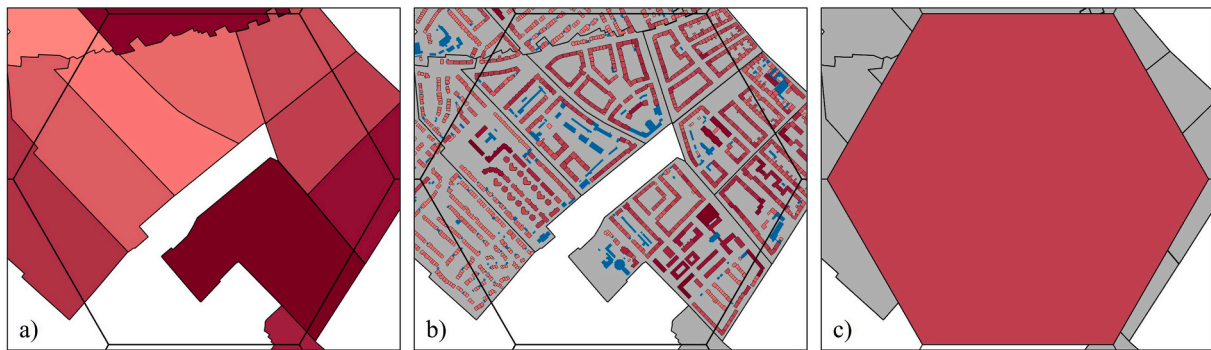


**Fig. 3.** Spatial level comparison for “total number of people”. a) Statistical district with socio-demographic information b) Base residence dataset with population disaggregated to residential buildings c) Hexagon with aggregated building information.

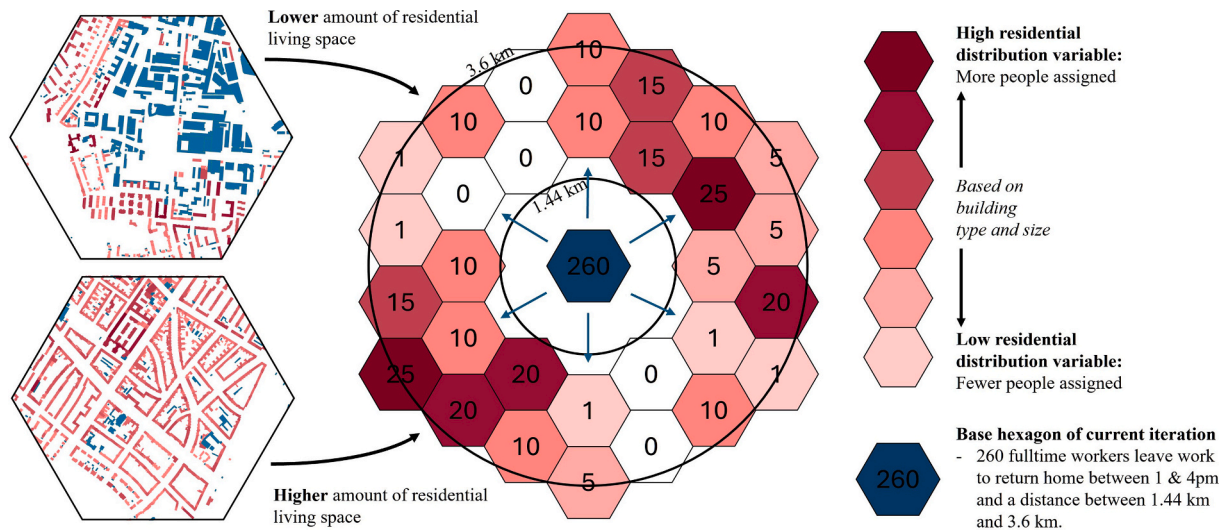


**Fig. 4.** Visualization of one distribution step for fulltime workers leaving work to return home. Exemplary scenario: 2400 fulltime workers work in the middle hexagon – between 1 pm – 4 pm, 260 of them travel between 1.44 km and 3.6 km (respectively 2 km and 5 km on nonlinear roads) to return home and get disaggregated depending on the hexagon’s amount of residential space (represented by the residential distribution variable derived from the buildings’ weights).

buildings with a low weight. The assigned people are then totaled per building, whereby the subgroups are retained.

**2.4. Step ④: inclusion of incoming commuters**

Commuters make up a large proportion of the full- and parttime workers in German cities. The Pendleratlas provides detailed numbers of commuters in and outflow for German municipalities (IT.NRW, 2024b). 402,476 people work and live in Cologne. An additional 362,259 people commute daily to Cologne, and another 172,509 leave the city to work (IT.NRW, 2024a). The outgoing commuters are already represented by the model. With 159,852, our modelling matches the figure of the

Pendleratlas by 93%. Commuters who come from outside and do not have a residence in the city are modelled separately. The number of incoming commuters is divided into 71% fulltime and 29% parttime workers (IT.NRW, 2024a). Afterwards, the activity profiles for fulltime and parttime workers are used to calculate how many commuters enter and leave the city at the different time intervals to work. These are then disaggregated to hexagon and building level via the work distribution variables (Table 7) of work buildings. This allows us to generate the same data structures and results as for the other subgroups, so that the commuters can be integrated seamlessly into the final model end product.

### 3. Results

The model results provide detailed information on the time-dependent location of the target city's population on several levels. On the spatial level, results are calculated on building, district, and hexagon level. For each of these levels, the information can be distinguished between the seven time intervals, the seven subgroups, the eleven activities, and combinations thereof. The following chapter compares the spatio-temporal results of our model to the static data that was available before. This allows us to understand the improvements made by our results. Subsequently, several validation strategies are illustrated to narrow down the strengths and weaknesses of the approach.

A secondary objective during the development of the model was to minimize computational effort. Using the hexagonal spatial calculation units greatly reduces the calculation time required. The city of Cologne has over 225,000 buildings and is divided into 438 hexagons, resulting in 1.18 million calculated trips at an overall calculation time of ca. 2 h on a mid-tier computer.

#### 3.1. Dynamic results in comparison to static maps

The visualization of the new data generated by our model shows significant differences from the previously available static maps. The static maps used as a comparison in the following figures are based on the SDC of Cologne dataset. It is available at district level, represents the highest resolution socio-demographic dataset publicly available for Cologne, and is comparable to similar datasets available for other cities. To ensure comparability with our results, the SDC population data is disaggregated to residential buildings for the building level based on floor area and story number. They are also re-aggregated to the hexagon level in line with our approach. These datasets represent the data status that was previously achievable before our model. Fig. 5 provides an overview of the result figure extents, a zoom-in on the city center of Cologne, and the main activity types, as well as the overall share of

square meters of each main activity type.

Fig. 6 shows the total number of people per hexagon without dividing by subgroups. This population density visualization shows that the static map is nearly equal to the modelled nighttime population, where most people are in the residential areas around the city center. Since most people are at home at night, this is consistent with the static map, which is based on official population registration data. During the day, however, our model uncovers different patterns. People leave the residential areas and move into the city center and towards outsourced work and industrial areas, which is in accordance with previous findings (Batista E Silva et al., 2020; Liu et al., 2018; Liu et al., 2021; Ma et al., 2017; Qi et al., 2015; Yoongsomporn et al., 2025).

The largest difference occurs between night or, respectively, the static version and midday in the city center, where the central hexagon of the modelling shows more than five times as many people as could be derived from the static data. But also, the main residential areas east and south-west of the city center show a great change in the number of present people by losing about half of their population (Fig. 7).

Fig. 8 shows the total number of people per building for the city center of Cologne without dividing it by subgroups. The spatially and temporally more fine-grained information that our model provides is particularly evident at the building level. The figure illustrates how buildings in the city center fill up over the course of the day with people going to work, shopping, or on private errands. Simultaneously, the smaller residential buildings empty steadily until the process reverses in the afternoon.

Table 8 provides an exemplary overview of the change in building population for different building types between nighttime and the static version compared to the afternoon, where the greatest differences occur. It has to be noted that people are only counted at the place of their respective activity. Traveling between two locations is not included. Overall, huge single buildings with a specialized usage type like sports arenas, train stations, or concert halls remain difficult to model adequately (Fig. 9).

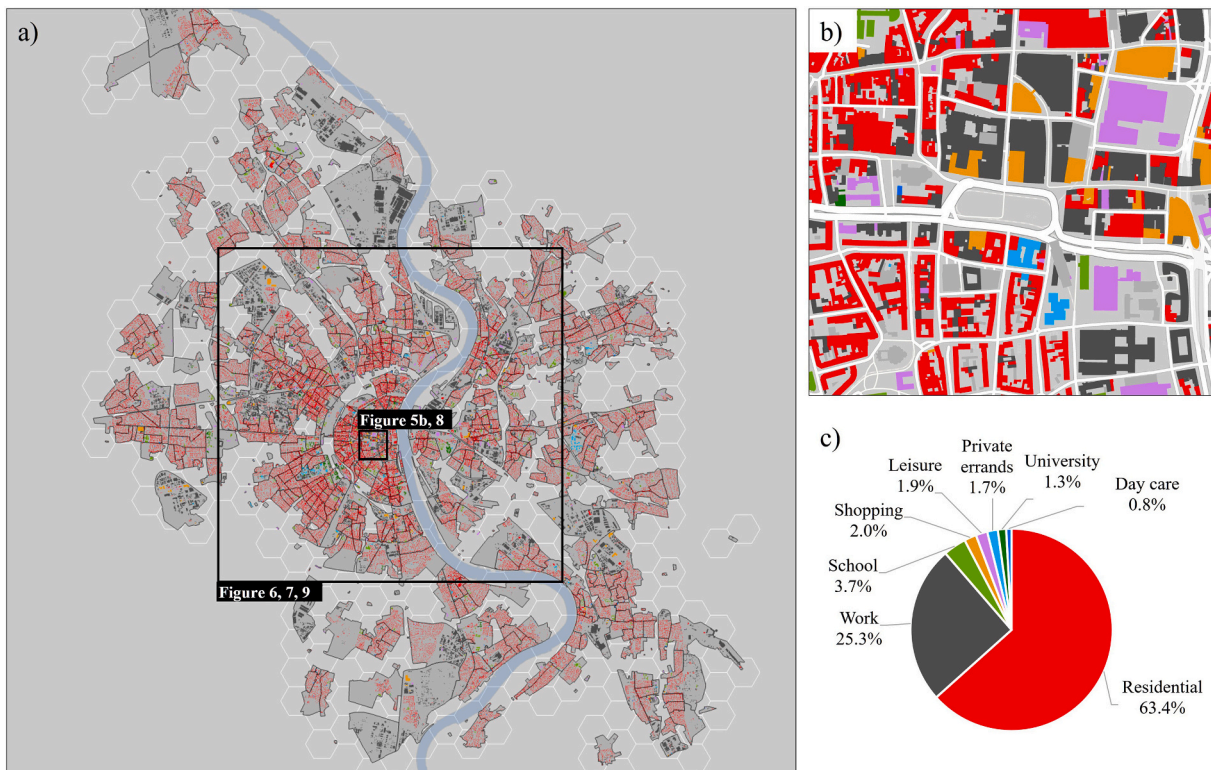


Fig. 5. Case study overview. a) City of Cologne with district and hexagon shapes; b) Section of Cologne city center with buildings color-coded by their main activity; c) Proportion of building area per building activity in Cologne.

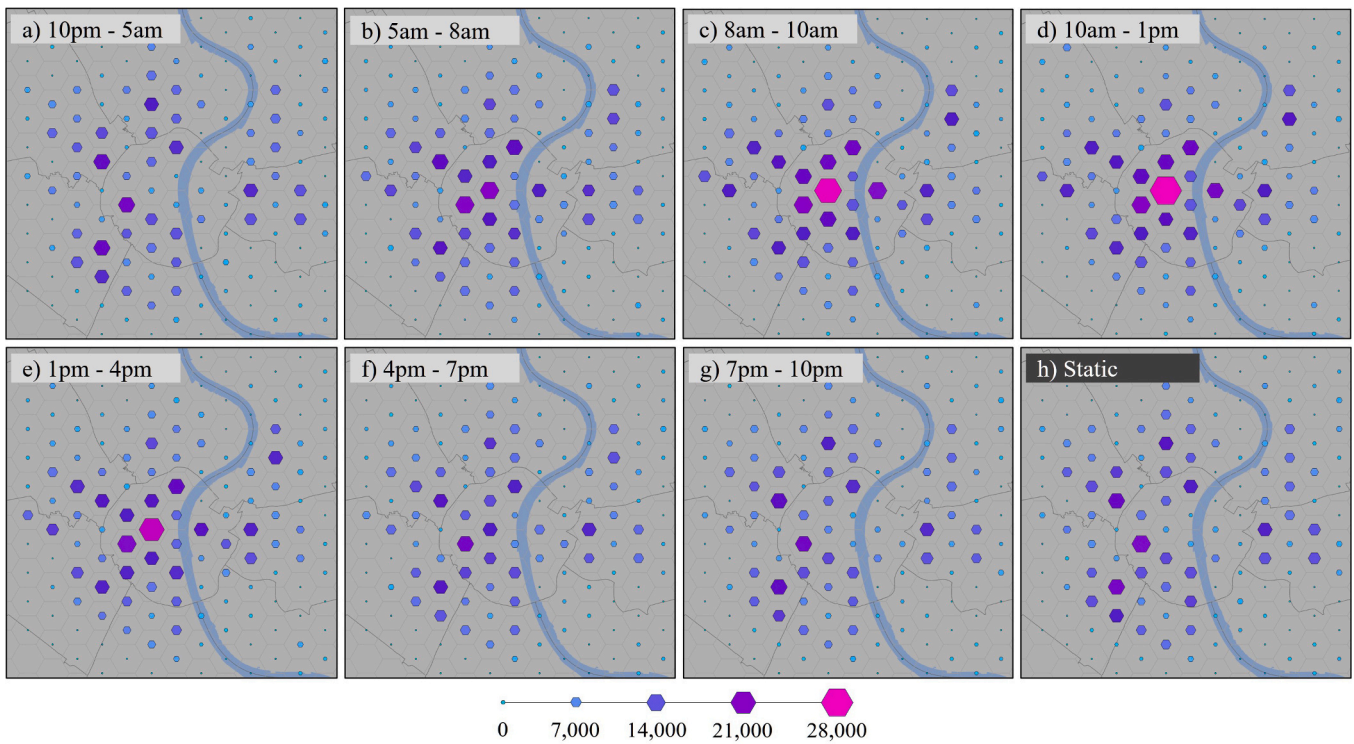


Fig. 6. Number of people per hexagon. a) - g) show the time-dependent model results; h) shows the previously available, static data, aggregated to hexagon level.

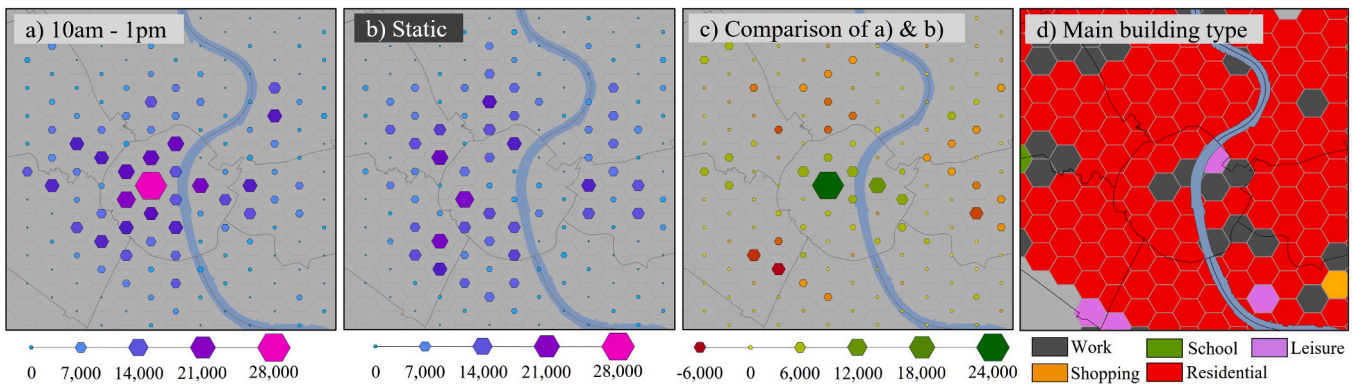


Fig. 7. Comparison of dynamic and static results on hexagon level. Absolute difference (c) per hexagon for the modelled midday result (a) and the previously existing static data version (b); (d) shows the most common building type per hexagon.

In contrast to many other spatio-temporal population models, our approach also distinguishes between seven population subgroups. This allows us to analyze the movement of specific social groups, such as more vulnerable groups of children and retired people. Fig. 10 shows the differences between static and dynamic data for total population, children, fulltime workers, and retired people. According to our model, children are focused on areas with more daycare centers, rather than residential areas like the static version suggests. This fits with the MiD information that most children are not at home during the first half of the day. While very few children are located in the city center during the day, it seems to be one of the focus points for the elderly population. The movement of this subgroup is influenced by shopping facilities and private errands such as doctors or hospitals, as well as the location of retirement homes. Full-time workers are strongly clustered during the day, with industrial parks, commercial areas (top left corner), industrial ports (top center), or the city center being particularly noticeable. The breakdown by subgroups shows the partially substantial differences in movement patterns between them. It also uncovers initially unintuitive

distributions, e.g., a substantial number of children in industrial and commercial areas, which is due to the fact that large companies sometimes have their own daycare centers. Such information can be vital, especially when it comes to the protection of vulnerable groups, and shows that a separate consideration of population groups is essential. It also underlines that population-based analyses, which are solely based on static data, can be subject to severe over- or underestimation over the course of a day.

### 3.2. Validation

The validation of spatio-temporal population models is challenging, as usually no suitable comparative data is available. Nevertheless, an analysis of the uncertainties is essential, especially for approaches that are not based on population movement measurements derived directly from reality (e.g., mobile phone locations). We first assess the base residence dataset created as input data in Step 2 for its correlation with static population data on building level to evaluate the disaggregation

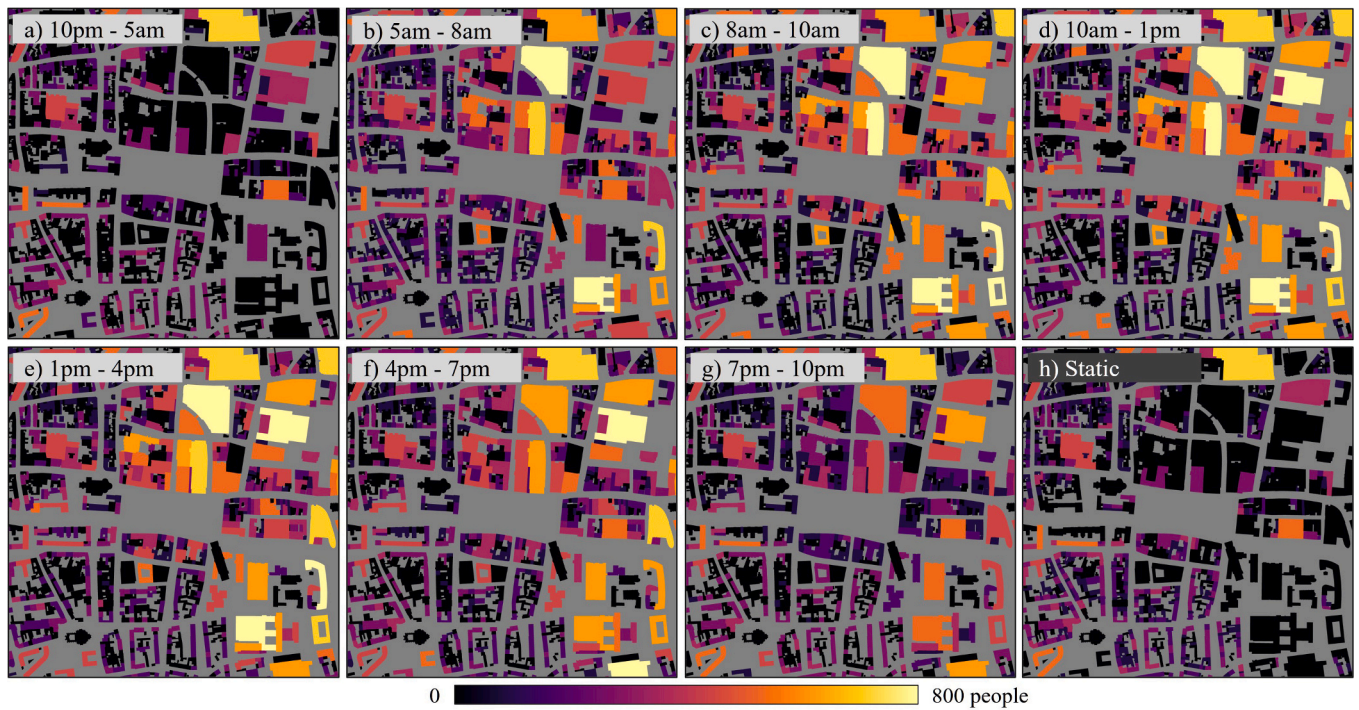


Fig. 8. Number of people per building. a) - g) show the time-dependent model results; h) shows the previously available, static data, aggregated to building level.

Table 8  
Detailed values per building.

No.	Building type	Category	No. of people in building		
			10 pm-5 am	10 am-1 pm	Static
1	Residential70	Residential building	20	8	16
2	Residential50_Work25	Residential building with commerce	9	4	8
3	Shopping100	Shopping center	0	618	0
4	Work87.5_Private25	Credit institute	0	168	0
5	Work62.5	Office building	0	734	0
6	Daycare100	Daycare for kids	0	43	0
7	School100	School	0	132	0



Fig. 9. Locations of buildings from Table 8.

method. Afterwards, we compare our model results with three fully independent datasets. First, the EU-wide available ENACT-POP (Schiavina et al., 2020) spatio-temporal population dataset published by the Joint Research Centre of the European Commission (Batista E Silva et al., 2020), followed by a comparison with an extensive emergency call dispatch dataset from Cologne. Finally, we compare our results to an hourly mobile phone location dataset for the city of Cologne.

### 3.2.1. Comparison of base residence dataset with high-resolution census

The base residence dataset (2.1. Step ①: Data preprocessing) is compared to a high-resolution population dataset, provided by the Office for Statistics of the City of Cologne. It includes the number of people registered for each residential building in Cologne, divided by demographic metrics. Comparability is hampered by the fact that some addresses have more than one building assigned. Our model allocates the associated people to all these buildings, whereas people in the validation dataset are only allocated to one building. We only compare those buildings that have people assigned in both datasets, which accounts for 80% of all residential buildings. This means that our results are constantly lower than the validation data, with a mean relative percentage error of 33%. The person correlation of 0.85 nevertheless shows a strong correlation with reality, and an R-squared value of 0.73 shows a high variation explanation. This proves that the methodology for creating the base residence dataset is suitable for preparing the model's base data.

### 3.2.2. Comparison of results with European day and night population dataset

For ENACT-POP, population counts from official census statistics are grouped into 16 population groups to estimate sub-national monthly and day- and nighttime population stocks for EU member states. These are dasymmetrically disaggregated based on land use and points of interest, resulting in a 1 km raster dataset, which provides monthly population counts for day and night based on data from 2011 (Batista E Silva et al., 2020). We chose the May dataset because this is an average month without holidays in Germany. We aggregate our 10 am - 1 pm (daytime), 10 pm - 5 am (nighttime) and the static data from building level to the 1

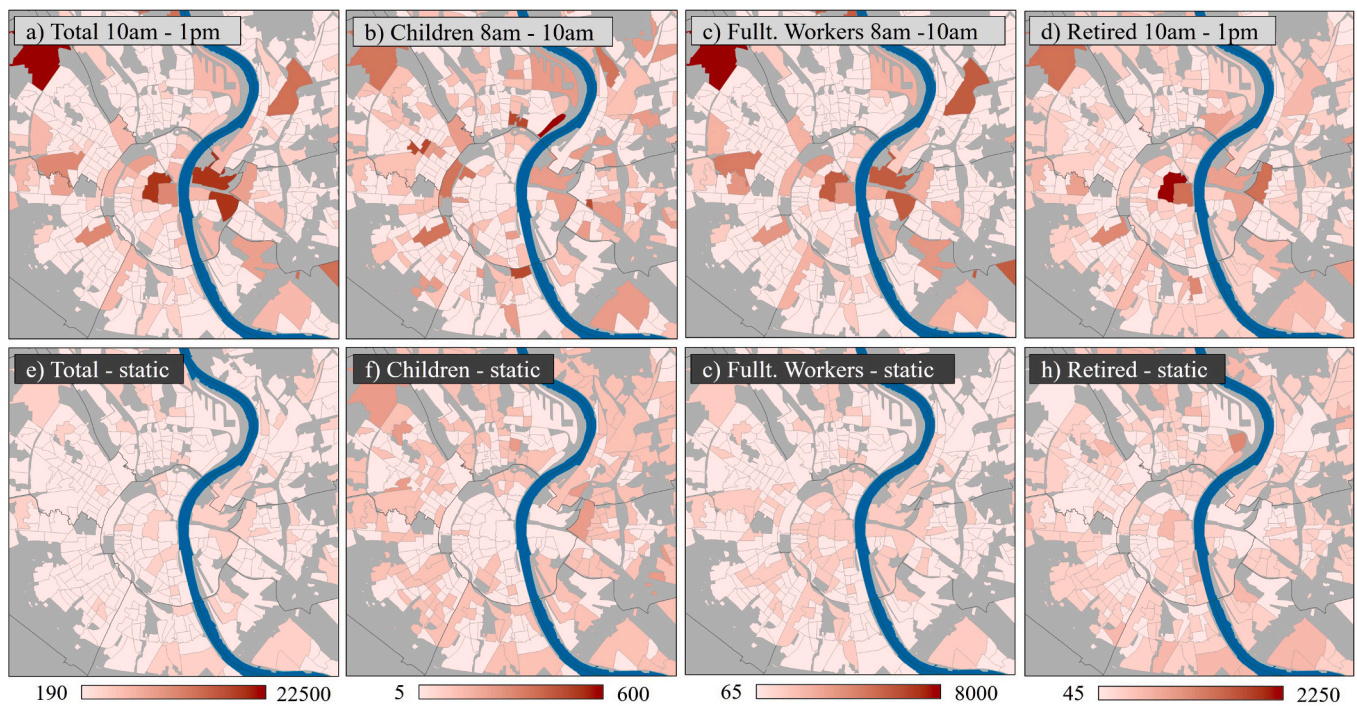


Fig. 10. Comparison of the day times with the highest activity and the static version for different subgroups. a) to d) display model results, e) to h) the static version.

Table 9

Results of Pearson correlation and linear regression analysis for the model results and the static data compared with the EU-wide available ENACT-POP day and nighttime dataset (Day: 10 am - 1 pm, night 10 pm - 5 am).

Time	99% of population 90th MAPE percentile				Static data			
	Model results				Static data			
	MAE	MAPE	Pearson	R <sup>2</sup>	MAE	MAPE	Pearson	R <sup>2</sup>
Day	1338	50.3%	0.86	0.74	1742	63.7%	0.75	0.57
Night	1201	59.2%	0.86	0.75	1293	63.6%	0.87	0.75

km ENACT-POP grid to compare both datasets and calculate the mean absolute error (MAE), the mean absolute percentage error (MAPE), Pearson correlation, and a linear regression analysis. Since some cells yield strong MAPE outliers due to empty cells, we cut off the highest 10% of the MAPE values, which accounts for less than 1% of the population. While at nighttime the our model reaches just slightly better results, we reach an overall 15% lower MAPE and higher correlation metrics during the day (Table 9), from which we conclude that our model offers an improved estimation of urban population mobility during the daytime.

### 3.2.3. Comparison of results with emergency calls

In the second validation approach, we use a different and fully independent dataset of emergency call locations from the fire department of Cologne. The dataset covers all dispatches of ambulance and fire service vehicles in Cologne for the years 2020, 2021, and 2023 (2022 had to be excluded due to corrupt location information). Per dispatch, the arrival time and emergency location are provided. This results in a spatio-temporal dataset of half a million points. We assume that, while emergency calls can certainly not fully explain daily population movements, those areas where many people are present should generate more emergency calls. A high correlation between emergencies and predicted number of present citizens would therefore point towards strong model accuracy. We divide the calls by time intervals, filter out weekends and public holidays, and summarize them per district. The district level is used for this analysis as its area is designed to cover the living area of

Table 10

Results of Pearson correlation and linear regression analysis for the model results and the static data compared with the number of emergency calls per city district.

Time	Model results		Static data	
	Pearson	R <sup>2</sup>	Pearson	R <sup>2</sup>
5 am–8 am	0.62	0.42	0.44	0.3
8 am–10 am	0.61	0.46	0.42	0.29
10 am–1 pm	0.64	0.5	0.38	0.28
1 pm–4 pm	0.64	0.53	0.36	0.3
4 pm–7 pm	0.66	0.5	0.37	0.3
7 pm–10 pm	0.61	0.44	0.41	0.32
10 pm–5 am	0.46	0.34	0.41	0.34

between 1000 and 3000 people, which makes them better suited for the comparison than the hexagons, which have strong variations in the total number of people. We calculate the Pearson correlation and a log-transformed linear regression analysis for the total number of people present per district and the number of emergencies for each time interval (Table 10). In comparison to the static results, our model consistently yields higher correlation coefficients across all time intervals, with values up to 0.66, while the static data features between 0.37 and 0.44 across all time intervals. Especially during the day, when most activity takes place, the model results improve, while the correlation with the static data declines. Also, the R<sup>2</sup> value is consistently higher, which

suggests that the time-dependent data explains up to three times more of the variation in emergency calls than the static counterpart. Even though our model outperforms the static data by far during the day, we reach equally low results during the night. A possible reason might be that the nighttime interval covers a longer period of seven hours, so that variations in emergencies cannot be considered properly. In addition, the type of emergencies could change at night. People being less active might lead to emergencies occurring for more randomly distributed reasons, which correlate less with the present number of people (e.g., a fire during night might be started by an electrical fault instead of cooking).

### 3.2.4. Comparison of results with mobile phone location data

Finally, we use population estimates based on mobile phone location data (MPLD) (purchased from invenium.io). The dataset provides the number of people per hour per 500 m grid cell for weeks 3 and 24 in 2024 in Cologne, from which we combine all working days. Based on mobile phone data from a company that has a 33% market share in Germany, it is determined how many phones are logged into each mobile phone cell tower in Cologne every hour. Using triangulation, the numbers from the towers are disaggregated to the 500 m grid cells. A 500 m resolution is the highest grid resolution that can be calculated while keeping the disaggregation inaccuracies maintainable. We compare the MLPD and the model results, both visually and statistically. While both datasets represent a derivation of reality, we treat the MLPD as “ground truth”, since it depicts real-world positioning data, which directly measures time-dependent population locations. Respective data limitations, necessary for the correct interpretation of the validation results, are covered in the following paragraphs, while the derived model limitations are addressed in the discussion chapter.

Fig. 11 shows a good visual consistency during day and night, with the distinction that the mobile phone data is more heterogeneous, with higher gradients between individual cells, while the model results look smoother. Closer examination reveals the overall spatial pattern changing more significantly in the model (e.g., city center), while the MPLD results keep a similar population pattern throughout day and night.

Further differences become apparent when viewed at the cell level. Our approach only assigns people to cells that contain buildings, while the MPLD results sometimes assign high values to cells that are close to built-up areas but are actually empty. On the other hand, the model fails to accurately represent night work and nightlife (Fig. 12). Special locations such as the main train station or sports arenas are also difficult to represent (Fig. 12). The MPLD partially has unrealistically strong cuts between neighboring cells, which may indicate the position of cell towers (Fig. 12).

Those differences lead to strong outliers with classical comparison metrics like the mean of the absolute errors per cell or the mean absolute percentage error. The highest MAPE outliers are mostly located in cells

with very low population. We therefore provide error metrics for the 80th and 35th MAPE percentile, which shows that the best 90% respectively 50% of the modelled population reach MAPEs of 54% and 24% and low MAEs, especially for midday, which we interpret as surprisingly high for data originating from two fundamentally different methods (Table 11).

### 3.3. Transfer to the city of Hamburg

To prove the model's transferability, we applied it to the city of Hamburg, Germany's second largest city with nearly two million inhabitants. The building and population data could be acquired via the geoportals of Hamburg and the neighboring federal states. Instead of small-scale statistical districts, we use larger city districts as the spatial unit for the population data in Hamburg to test the impact on the results. In the model, we only adjusted the calculation of the seven subgroups, since the socio-demographic data provided for Hamburg is slightly different.

Comparison with the ENACT-POP dataset and our model results for 10 am – 1 pm show a Pearson correlation of 0.81 with an  $R^2$  of 0.65 for the model, and a correlation of 0.77 with an  $R^2$  of 0.59 for the static version. This is in line with the values from the model validation for Cologne (Table 9) and suggests a successful transfer. The slight decrease in correlation is likely due to the higher size and heterogeneity of the district-based input data of Hamburg.

This transfer to Hamburg demonstrates that our model is applicable to a distinct administrative entity with different municipal data portals and infrastructure. Since data portals of major German cities are similar in structure and data offers, this underlines the model's transferability to other cities.

## 4. Discussion

The main objective of this paper was to develop a model that is able to close the data gap for urban population maps in terms of spatio-temporal population dynamics for German main cities. The presented model is able to achieve results with a high spatial and temporal resolution while at the same time differentiating between socio-demographic population groups, as well as maintaining a high transferability. Finally, sufficient validation of the results could be presented.

### 4.1. Discussion of results

Comparing the previously available static population maps for the case study of Cologne with the seven time-dependent population maps from our model, we are able to demonstrate that severe differences in the daily population distribution can be uncovered by the model's results. Taking the city center hexagon as an example, where around 4000 people are located according to static data, while the dynamic data

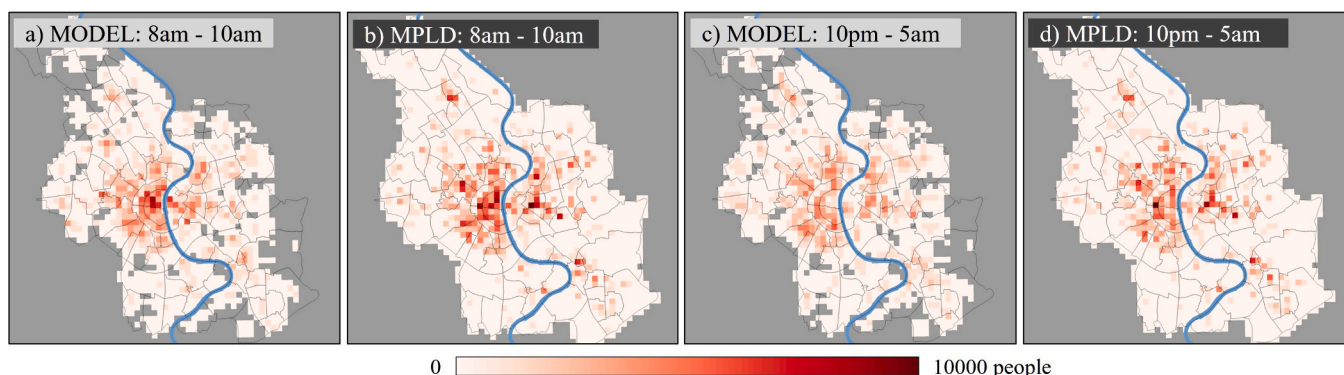


Fig. 11. Visual comparison of the model results and mobile phone-based population estimations.

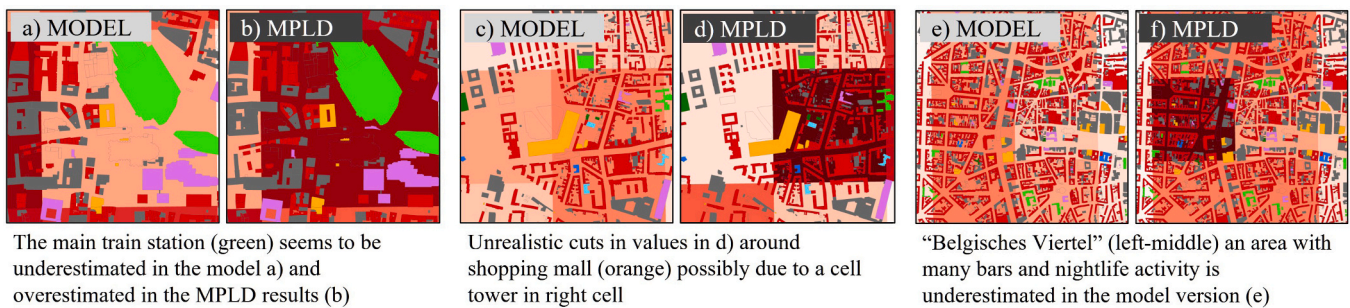


Fig. 12. Exemplary detailed comparison of the model and mobile phone-based results.

**Table 11**  
Comparative metrics for the model results and mobile phone-based results.

Time	90% of population 80th MAPE percentile			50% of population 35th MAPE percentile		
	MAE	MAPE	Pearson	MAE	MAPE	Pearson
	5 am–8 am	–183.9	0.54	0.81	–90.9	0.24
8 am–10 am	–86.2	0.54	0.81	–41.1	0.24	0.94
10 am–1 pm	–27.2	0.55	0.83	–36.1	0.25	0.92
1 pm–4 pm	–13.6	0.55	0.83	–34.1	0.24	0.94
4 pm–7 pm	–8	0.56	0.85	–21.8	0.26	0.93
7 pm–10 pm	–42.5	0.57	0.83	–10.9	0.26	0.92
10 pm–5 am	–116.5	0.59	0.79	–39.6	0.27	0.91

reveals a peak of up to 24,000 people being actually present at the late morning. This proves how crucial spatio-temporal population data is for a wide range of applications, especially in emergency situations. The division into subgroups allows an even finer distinction of population localization. It allows us to identify subgroup-specific movement patterns that cannot be derived from static data but are crucial for vulnerability analyses. The transfer case study of Hamburg confirms that our model is transferable to other cities in Germany. This is possible due to the model only using publicly and Germany wide available data. The validation with spatio-temporal population maps of an independent approach (Batista E Silva et al., 2020) detailed emergency call data and mobile phone positioning data also suggest a high degree of accuracy of the generated data. Overall, the validation proves a substantial improvement in the population representation by our dynamic data in comparison to static data. In comparison with the ENACT-POP dataset, the, to our knowledge, only other spatio-temporal data set that covers Germany, we can achieve higher spatial (building vs. 1 km grid) and temporal (two vs. seven time intervals) resolution, while implementing updated input data (2011 vs 2023). This underlines the improvements achieved by our approach and shows that the data landscape in Germany is indeed comprehensive and detailed enough to serve as a basis for dasymetric spatio-temporal population models and yield usable results.

#### 4.2. Comparison with existing spatio-temporal population models

Building upon the overview of similar models in the introduction, we focus on comparing the methodologies and results in this chapter. We choose major models, developed in the last ten years, that also follow the dasymetric method direction instead of using real-world positioning data, and are therefore methodology-wise relatable to our approach.

The LandScanHD approach by Tuccillo et al. (2025) is designed for global application. It combines the bottom-up assignment of occupancy weights to buildings with top-down redistribution of official population counts. The difference between day and nighttime occupancy is based on the ORNL's Population Density Tables project, which uses observations and subject matter expertise on facility occupancy throughout the world, in combination with a Bayesian machine learning approach

(Stewart et al., 2016) to develop occupancy rates for 50 building types (Urban et al., 2023). While this approach is developed for global application, our localized, but rich data environment enables us to develop weights for 235 buildings instead, which are based on official building descriptions. The model further includes mobility information, meaning that population behavior and building location are taken into account, which severely improves our results.

For the ENACT-POP dataset, Batista E Silva et al. (2020) divide the EU population into 16 activity-related groups on country province level (NUTS3) for each month of the year. Consequently, various land use, land cover, and points of interest information are used to dasymetrically disaggregate the population groups to 100 m grid cells. Day and night differences are achieved by adding up different population classes. The result comprises a monthly EU-wide 1 km grid with day and night population for the year 2011. One difference between our approach and theirs is that, in order to achieve greater coverage, they work with much coarser input data (province vs. district), which allows our model to achieve greater precision at the city level. We also use mobility information, which allows for greater temporal resolution and acts as an additional component in population allocation.

Our approach shares many characteristics with the spatio-temporal population model framework developed by Martin et al. (2015). The respective Population24/7 dataset (Cockings et al., 2021) provides population estimates for 2 am and 2 pm for a typical weekday in and out of termtime in the UK. Workplace statistics and census area centroids, specific location data (e.g., hospitals, schools), and roads are used to generate origin and destination containers. Activity profiles for seven population groups in combination with capacity curves for the destination containers are used to assign population in 15 min steps. The results are provided at a 200 m grid level. Unlike our approach, Population24/7 has a flexible temporal resolution and includes the traveling population. By utilizing capacity values for the destinations, Population24/7 prevents “over-assignment” to cells, which we cannot control in our destination buildings. Our detailed building data set and disaggregation method, on the other hand, allow us to make a building-level assignment of the starting population and arriving population, instead of the assignment to census area centroids. We also take into account that a person often performs more than one activity per day, which better reflects population behavior. Additionally, we managed to include different travel distances per activity, which was already suggested as a possible improvement in Martin et al. (2015).

While LandScanHD and ENACT-POP have the advantage of being transferable beyond the national level, our approach achieves greater accuracy by focusing on a data-rich region. Among other things, this makes it possible to include mobility information such as travel distances and the number of daily activities and precise building data, resulting in higher spatial and temporal resolution. Population24/7 and the approaches based on it (Pittore et al., 2023; Renner et al., 2018; Smith et al., 2016) follow the most similar approach to our model. While the model is limited to urban areas and does not yet include traveling between destinations, we manage to include more mobility information

**Table 12**  
Comparison of the model output of recent spatio-temporal population datasets.

Source	Model name	Data year	Spatial resolution	Temporal resolution	Population subdivision	Area covered
Tuccillo et al. (2025)	LandsatHD	varying	100 m grid	Day/night	–	Global, specific countries
Batista E Silva et al. (2020)	ENACT-POP	2011	1 km grid	Day/night	–	EU
Cockings et al. (2021)	Population 24/7	2011	200 m grid	Day/night (More is possible)	Seven population groups	UK
Smith et al. (2016)	Based on Population 24/7	2000–2006	200 m grid	Hourly	Seven population groups	Southampton, UK
Renner et al. (2018)	Based on Population 24/7	2015	100 m grid	Hourly	Residents, Workers, Students, Tourists	Bolzano, South Tyrol, Italy
Pittore et al. (2023)	Based on Population 24/7	2022	250 m hexagon	Day/night, commuting	Residents, workers	Bolzano, South Tyrol, Italy
This paper	–	2023	Building level	8 am, 10 am, 1 pm, 4 pm, 7 pm, 10 pm, 5 am	Seven population groups	Cologne; transferable to German main cities

and a finer population assignment in our method, which is partly due to the improved data available today.

Table 12 provides an additional overview of the result metrics of the previous spatio-temporal population models. The comparison shows that our model can reach convincing metrics in terms of spatial and temporal resolution. It also underlines that a future challenge will be to transfer the model beyond Germany.

#### 4.3. Limitations of the model

In this section, we discuss the remaining limitations of our model. While we could validate the aggregated results on the hexagon and district level, we are not aware of any dataset to conduct a validation on the building level. We receive the building-level results by disaggregating the hexagon level with our distribution variable-based method. Since this method has been successfully validated in chapter 3.2.1 “Comparison of base residence dataset with high-resolution census”, as working sufficiently, we assume that the final results are also credible. In addition, the data sets for validation of the final results were created by aggregating the building data set, which led to the satisfactory validation results described above. Nevertheless, even if most of the individual population counts per building seem realistic at visual inspection, we cannot provide exact uncertainty metrics, which have to be taken into account when using the data. Despite this, we decided to provide the results at the building level, since this data resolution allows us to aggregate the results to various spatial shapes. This is relevant for cases where dynamic population data needs to be combined with complex geodata like hazard maps. It also helps to counter the modifiable aerial unit problem (Openshaw, 1984).

While the validation of the total number of people was successful at the district level, we are missing data to validate the seven subgroups independently, both at building and district level. Manual assessments of individual numbers, however, show credible values in most cases. The validation results of the total population also suggest that at least the subgroup of workers, which has the highest proportion of the total population, is correctly estimated. Nevertheless, the subgroup results should therefore be used with caution.

In terms of the activity profiles, our model is restricted to the information from the MiD study. This leads to restrictions, like only assigning one activity per person per time interval, and the assumption that the first activity during a day is the main activity. While this has to be accepted now, the model's structure allows for easy implementation of more detailed mobility information in the future.

Our approach does not take the traveling between locations into account. This can lead to underestimations in either highly traveller-frequented locations like train stations or tourist areas, as well as main roads and public transport during peak hours. In highly frequented areas, like the inner city, this problem might be less severe, once the

results are used above the level of single buildings – e.g., if the population counts are aggregated at the block level, which includes several buildings and roads, the population numbers per building compensate partially for the adjacent roads. However, this effect cannot be quantified due to a lack of data. In non-built-up areas, with main roads or public transport lines, this limitation can not be compensated at all, which has to be taken into account when using the result data, especially for disaster risk assessment. We plan to improve the model in the future by adding “traversing” as time dependent activity for all subgroups and including OpenStreetMap roads, with a type-dependent capacity, similar to the buildings. This would allow to estimate the traveling population, while still fitting in the existing model framework and maintaining transferability.

Our approach models a standard workday and is built on average statistical values. This makes it highly versatile, transferable, and usable with publicly available data, but results in problems for “out of the average” situations. Weekends and public holidays can therefore be represented less well by our model as long as no information about the changed mobility behavior is available. For the future, the inclusion of city-specific tourism data is planned.

We further see unrealistic model results for single, specialized buildings like sports arenas and event locations with irregular occupancy rates, since our approach provides an average number of present people and cannot cover such irregular peaks. We decided against the use of building-specific event schedule information to maintain transferability of the model.

#### 4.4. Future transfer to other countries

The model is developed and tested for the data-rich region of Germany. Nevertheless, the approach offers potential for expansion to other countries. This requires similar socio-demographic data, building data, and mobility information, which essentially limits it to data-rich regions. In the following, we discuss data needs for these three domains, as well as potential datasets, to provide a first impression of model transfer opportunities and to locate upcoming difficulties that would need to be addressed in further research.

Socio-demographic data is usually collected in some form of census survey in data-rich regions. These differ from country to country or even city to city in terms of characteristics and spatial resolution. For our model, population characteristics must be distinct enough to allow the population to be divided into activity-related subgroups. Since this can be achieved in various ways, using a variety of common characteristics, such as age distributions, we expect this to be achievable. Spatial resolution poses a greater problem. In order to obtain reliable model results at the building level, the input data must be of sufficiently high-resolution for the disaggregation to remain meaningful. If this is not the case, an alternative approach could be to ignore the building level

and work on the hexagon level, whereby the level of disaggregation can be adjusted by the hexagon size.

On the building side, geodata on building floor space and height, as well as detailed building usage data, are essential. While impressive progress has been made in recent years in terms of data on building footprints and height (Pesaresi et al., 2024), most recently with the Global Building Atlas (Zhu et al., 2025), which provides polygons and height information for 2.75 trillion building polygons, there is still a lack of global datasets providing information on building usage. The use of land use (Schultz et al., 2024) data could pose an alternative, but would likely lead to results in lower resolution. Country-specific datasets such as CMAB (Zhang et al., 2025), could be a high-resolution alternative.

In the field of mobility information, there are promising studies at the national level for data-rich regions, including Norway, Sweden, Denmark, England, and France (Gunnhild et al., 2024) and the US (U.S. Department of Transportation, 2022). These studies differ in terms of study design and methodology, which precludes direct transferability. However, since the aim of all these studies is to comprehensively describe the mobility behavior of the national population, it is reasonable to assume that the necessary mobility metrics could also be calculated from these studies.

The model can, in principle, be transferred to all regions for which the appropriate data is available. The varying data availability and nature of data sets in all areas make it impossible to make a universal statement. Instead, it must be checked individually for each region whether suitable data is available, which would go beyond the scope of this paper.

This approach is tailored to data-rich regions that collect and publish extensive information on population, buildings, and mobility. This limits the usability of the approach in data-poor regions. Nevertheless, a global upward trend in data collection and publication can be observed (Gao et al., 2023; Herfort et al., 2023), which suggests that more regions provide the necessary data in the future. Another advantage is the model's flexibility in terms of input data, as regional data with different building types, activity groups, or spatial resolutions (building or hexagon level) can be easily used with this approach. Further, the use of machine learning or deep learning methods in conjunction with the globally improving data situation (building information, land use, nighttime lights, census data, global population maps, OpenStreetMap data, etc.) could offer new opportunities (Gunkel et al., 2025; Urban et al., 2023; Xie et al., 2020) to estimate time-dependent population location based on model results from data-rich regions.

#### 4.5. Demand for spatio-temporal population data

The differences uncovered between dynamic and static population data in Cologne of up to 600% inevitably raise the question of how reliable population-based analyses can be if they do not take the time component into account. Mostly in approaches, where the population is analyzed at a specific point in time, serious misestimations would have to be expected. This confirms again what previous research pointed out, that the temporal component plays an enormous role in population data (Ahola et al., 2007; Freire et al., 2013; Freire & Aubrecht, 2012; Pittore et al., 2017; Pittore et al., 2023; Renner et al., 2018; Smith et al., 2016). We therefore join the call for more dynamic population data that considers a time-of-day component.

We further want to add two needs to this call. First, for approaches that are transferable and cover wide areas, instead of methods that generate data only for small areas or single cities. Second, for the increased public availability of such data. There are two datasets known to the authors so far that fulfill both criteria. The ENACT-POP dataset from Batista E Silva et al. (2020) provides day and night population for Europe on a 1 km grid, based on data from 2011, which was used to validate our model. The Population 24/7 model from Cockings et al. (2021) covers the UK and is based on 2011 data. We believe that both criteria have to be fulfilled to reduce the hurdle in the use of spatio-

temporal data to such an extent that it will be broadly applied.

Positioning data-based approaches have so far been the predominant option to generate spatio-temporal population data, although they are usually expensive and might underrepresent certain population groups. Dasymeric approaches, which instead combine geodata with static demographic data and model the population mobility based on mobility information (e.g. surveys), need extensive amounts of heterogeneous high-resolution data to reach similar results, which was often challenging in the past. Our approach demonstrates that the open data landscape in data-rich regions like Germany is, in the meantime, sufficient enough to develop dasymeric models that reach such quality levels that they pose a serious alternative to positioning data-based approaches, especially considering that they are based on publicly available data.

## 5. Conclusion

In this paper, we introduced a spatio-temporal population model for major cities in Germany. The model uses publicly available population and building data in combination with mobility survey results to calculate population maps for seven time intervals throughout one day. Each map provides the number of people, divided into seven activity-related subgroups, per building. This advance from static to dynamic spatio-temporal data significantly increases the accuracy of population mapping. Comparisons of city districts in the city of Cologne show that traditional static population data underestimates population figures up to five times and overestimates up to two times during certain times of day. These findings underscore the limitations of static population data and show the need for the inclusion of the temporal dimension in population mapping, particularly in time-sensitive contexts like emergency management or risk analyses for sudden onset disasters. Since our results are also provided at the level of population subgroups, such as children or retired people, the temporal component of vulnerable groups can be taken into account, which makes our dataset particularly suitable for disaster management and risk analyses.

The model results have undergone a threefold validation procedure by analysing the correlation with three independent datasets. In comparison with the ENACT Pop dataset, which is available throughout Europe but has a coarser resolution, an extensive emergency call dataset, as well as a time-of-day-dependent dataset of mobile phone positions, our results show good reliability and realistic representation of spatio-temporal reality. Especially during the daytime, our results heavily outperform traditional static data.

By relying exclusively on data that is available throughout all major German cities, our model is developed to be transferred beyond the initial case study of Cologne. The successful application to the city of Hamburg validates this adaptability.

With the high spatial and temporal resolution that could be successfully validated, as well as the possibility of transfer to other cities, we conclude that the model contributes significantly to closing the gap in dynamic population data for Germany. An extension of the model to other cities and countries is planned for the future. Our approach also underscores the chances Germany's extensive open data landscape provides for population modelling. Building on such a data foundation, such dasymeric modelling approaches provide competitive alternatives to approaches that rely on often expensive positioning data like mobile phone locations.

## CRedit authorship contribution statement

**Peter Priesmeier:** Writing – review & editing, Writing – original draft, Visualization, Validation, Software, Methodology, Investigation, Formal analysis, Data curation, Conceptualization. **Alexander Fekete:** Writing – review & editing, Supervision, Resources, Conceptualization. **Michael Haberl:** Writing – review & editing, Validation, Data curation. **Christian Geiß:** Writing – review & editing, Supervision,

Conceptualization. **Roland Baumhauer**: Writing – review & editing, Supervision, Conceptualization. **Hannes Taubenböck**: Writing – review & editing, Supervision, Conceptualization.

**Funding**

This research did not receive any specific grant from funding agencies in the public, commercial, or not-for-profit sectors.

**Declaration of competing interest**

Peter Priesmeier: The author has declared that no competing interests exist.

Alexander Fekete: The author has declared that no competing interests exist.

Christian Geiß: The author has declared that no competing interests exist.

Michael Haberl: This study was supported through data provision by Invenium Data Insights. The company had no involvement in the analysis or interpretation of the findings.

Roland Baumhauer: The author has declared that no competing interests exist.

Hannes Taubenböck: The author has declared that no competing interests exist.

**Appendix A. Data tables**

**Table A1**  
Share of daily activities for children.

Children	Primary	Secondary
1 + 2 Trips	38%	0%
3 + 4 Trips	36%	36%
5+ Trips	15%	30%
Total	89%	66%
Stay home (0 Trips)	11%	

**Table A2**  
Share of daily activities for pupils.

Pupils	Primary	Secondary
1 + 2 Trips	39%	0%
3 + 4 Trips	36%	36%
5+ Trips	16%	32%
Total	91%	68%
Stay home (0 Trips)	9%	

**Table A3**  
Share of daily activities for students.

Students	Primary	Secondary
1 + 2 Trips	32%	0%
3 + 4 Trips	33%	33%
5+ Trips	22%	44%
Total	87%	77%
Stay home (0 Trips)	13%	

**Table A4**  
Share of daily activities for fulltime.

Fulltime	Primary	Secondary
1 + 2 Trips	38%	0%
3 + 4 Trips	32%	32%
5+ Trips	20%	40%
Total	90%	72%
Stay home (0 Trips)	10%	

**Table A5**  
Share of daily activities for parttime.

Parttime	Primary	Secondary
1 + 2 Trips	28%	0%
3 + 4 Trips	32%	32%
5+ Trips	32%	64%
Total	92%	96%
Stay home (0 Trips)	8%	

**Table A6**  
Share of daily activities for jobless.

Jobless	Secondary I	Secondary II
1 + 2 Trips	31%	0%
3 + 4 Trips	27%	27%
5+ Trips	21%	42%
Total	79%	69%
Stay home (0 Trips)	21%	

**Table A7**  
Share of daily activities for retired.

Retired	Secondary I	Secondary II
1 + 2 Trips	35%	0%
3 + 4 Trips	28%	28%
5+ Trips	17%	34%
Total	80%	62%
Stay home (0 Trips)	20%	

**Acknowledgements**

We thank Abteilung Statistik und Informationsmanagement of the

City of Cologne and the Amt für Feuerschutz, Rettungsdienst und Bevölkerungsschutz of the City of Cologne for their support with the third-party data.

**Table A8**  
Activity profile for “Children”.

Children Time	Home	To Day care	From Day care	To Shopping	From Shopping	To Private	From Private	To Leisure Res	From Leisure Res	To Leisure Genrl	From Leisure Genrl	To Leisure Sport	From Leisure Sport	To Leisure OutG	From Leisure OutG
5 am–8 am	70.0%	29.37%	0.00%	0.32%	0.00%	0.22%	0.07%	0.09%	0.00%	0.00%	0.00%	0.00%	0.00%	0.00%	0.00%
8 am–10 am	12.8%	53.40%	2.67%	3.07%	0.32%	2.32%	0.22%	0.64%	0.09%	0.63%	0.00%	0.02%	0.00%	0.03%	0.00%
10 am–1 pm	14.3%	1.78%	13.35%	4.69%	3.07%	1.95%	2.32%	2.10%	0.64%	4.21%	0.63%	0.46%	0.02%	0.74%	0.03%
1 pm–4 pm	34.6%	3.56%	27.59%	3.07%	4.69%	1.95%	1.95%	3.56%	2.10%	7.05%	4.21%	0.86%	0.46%	1.38%	0.74%
4 pm–7 pm	72.1%	0.89%	35.60%	4.53%	3.07%	0.90%	1.95%	2.65%	3.56%	3.97%	7.05%	0.48%	0.86%	0.77%	1.38%
7 pm–10 pm	97.2%	0.00%	8.90%	0.32%	4.53%	0.00%	0.90%	0.18%	2.65%	0.79%	3.97%	0.08%	0.48%	0.12%	0.77%
10 pm–5 am	99.9%	0.00%	0.89%	0.00%	0.32%	0.07%	0.00%	0.00%	0.18%	0.00%	0.79%	0.00%	0.08%	0.00%	0.12%

**Table A9**  
Activity profile for “Pupils”.

Pupils Time	Home	To School	From School	To Shopping	From Shopping	To Private	From Private	To Leisure Res	From Leisure Res	To Leisure Genrl	From Leisure Genrl	To Leisure Sport	From Leisure Sport	To Leisure OutG	From Leisure OutG
5 am–8 am	33.0%	66.43%	0.00%	0.24%	0.12%	0.06%	0.06%	0.02%	0.09%	0.07%	0.28%	0.17%	0.17%	0.00%	0.15%
8 am–10 am	13.1%	18.20%	0.91%	0.80%	0.24%	0.17%	0.06%	0.09%	0.02%	1.04%	0.07%	0.84%	0.17%	0.00%	0.00%
10 am–1 pm	15.2%	1.82%	10.01%	3.13%	0.80%	0.83%	0.17%	0.56%	0.09%	1.58%	1.04%	1.69%	0.84%	0.66%	0.00%
1 pm–4 pm	40.5%	3.64%	36.40%	4.81%	3.13%	1.22%	0.83%	0.95%	0.56%	3.20%	1.58%	3.71%	1.69%	0.95%	0.66%
4 pm–7 pm	57.3%	0.91%	28.21%	5.97%	4.81%	2.11%	1.22%	1.47%	0.95%	6.36%	3.20%	8.43%	3.71%	1.02%	0.95%
7 pm–10 pm	87.3%	0.00%	12.74%	1.98%	5.97%	1.11%	2.11%	0.90%	1.47%	2.32%	6.36%	1.86%	8.43%	0.88%	1.02%
10 pm–5 am	99.0%	0.00%	2.73%	0.12%	1.98%	0.06%	1.11%	0.09%	0.90%	0.28%	2.32%	0.17%	1.86%	0.15%	0.88%

**Table A10**  
Activity profile for “Students”.

Students Time	Home	To University	From University	To Shopping	From Shopping	To Private	From Private	To Leisure Res	From Leisure Res	To Leisure Genrl	From Leisure Genrl	To Leisure Sport	From Leisure Sport	To Leisure OutG	From Leisure OutG
5 am–8 am	90.9%	9.57%	0.87%	0.05%	0.28%	0.13%	0.15%	0.01%	0.72%	0.05%	0.15%	0.10%	0.10%	0.00%	0.43%
8 am–10 am	57.7%	32.19%	2.61%	1.71%	0.05%	0.32%	0.13%	0.30%	0.01%	0.36%	0.05%	0.91%	0.10%	0.11%	0.00%
10 am–1 pm	30.6%	26.97%	10.44%	6.21%	1.71%	1.22%	0.32%	2.11%	0.30%	1.19%	0.36%	2.02%	0.91%	1.09%	0.11%
1 pm–4 pm	31.5%	13.92%	17.40%	6.10%	6.21%	1.51%	1.22%	3.44%	2.11%	1.74%	1.19%	1.82%	2.02%	0.87%	1.09%
4 pm–7 pm	47.5%	4.35%	26.97%	7.13%	6.10%	2.23%	1.51%	4.76%	3.44%	2.64%	1.74%	3.44%	1.82%	1.52%	0.87%
7 pm–10 pm	73.9%	0.00%	17.40%	2.87%	7.13%	1.82%	2.23%	3.66%	4.76%	1.78%	2.64%	1.72%	3.44%	1.41%	1.52%
10 pm–5 am	97.7%	0.00%	11.31%	0.28%	2.87%	0.15%	1.82%	0.72%	3.66%	0.15%	1.78%	0.10%	1.72%	0.43%	1.41%

**Table A11**  
Activity profile for “Fulltime Workers”.

Fulltime Time	Home	To Work	From Work	To Shopping	From Shopping	To Private	From Private	To Leisure Res	From Leisure Res	To Leisure Genrl	From Leisure Genrl	To Leisure Sport	From Leisure Sport	To Leisure OutG	From Leisure OutG
5 am–8 am	46.61%	51.30%	1.80%	0,80%	0,04%	0,23%	0,07%	0,03%	0,01%	0,16%	0,50%	0,36%	0,07%	0,00%	0,33%
8 am–10 am	23.05%	22.50%	3.60%	3,42%	0,80%	1,15%	0,23%	0,15%	0,03%	0,61%	0,16%	0,50%	0,36%	0,14%	0,00%
10 am–1 pm	17.27%	5.40%	8.10%	6,75%	3,42%	1,99%	1,15%	0,40%	0,15%	2,72%	0,61%	1,14%	0,50%	0,80%	0,14%
1 pm–4 pm	29.34%	5.40%	17.10%	5,51%	6,75%	1,75%	1,99%	0,40%	0,40%	3,55%	2,72%	1,07%	1,14%	0,66%	0,80%
4 pm–7 pm	55.64%	1.80%	36.00%	8,22%	5,51%	2,19%	1,75%	0,48%	0,40%	5,14%	3,55%	2,77%	1,07%	1,60%	0,66%
7 pm–10 pm	84.66%	1.80%	17.10%	1,89%	8,22%	0,48%	2,19%	0,15%	0,48%	2,78%	5,14%	1,28%	2,77%	1,13%	1,60%
10 pm–5 am	96.93%	1.80%	6.30%	0,04%	1,89%	0,07%	0,48%	0,01%	0,15%	0,50%	2,78%	0,07%	1,28%	0,33%	1,13%

**Table A12**  
Activity profile for “Parttime Workers”.

Parttime Time	Home	To Work	From Work	To Shopping	From Shopping	To Private	From Private	To Leisure Res	From Leisure Res	To Leisure Genrl	From Leisure Genrl	To Leisure Sport	From Leisure Sport	To Leisure OutG	From Leisure OutG
5 am–8 am	61.0%	35.88%	0.92%	1.00%	0.00%	0.29%	0.04%	0.03%	0.03%	0.07%	0.62%	0.15%	0.08%	0.00%	0.20%
8 am–10 am	24.4%	32.20%	4.60%	5.20%	1.00%	1.80%	0.29%	0.32%	0.03%	1.04%	0.07%	0.99%	0.15%	0.15%	0.00%
10 am–1 pm	18.3%	10.12%	14.72%	9.68%	5.20%	3.02%	1.80%	0.76%	0.32%	3.96%	1.04%	1.44%	0.99%	0.80%	0.15%
1 pm–4 pm	31.8%	8.28%	23.92%	9.44%	9.68%	2.69%	3.02%	0.80%	0.76%	5.67%	3.96%	1.44%	1.44%	1.00%	0.80%
4 pm–7 pm	55.6%	2.76%	28.52%	9.24%	9.44%	2.49%	2.69%	0.64%	0.80%	6.09%	5.67%	2.20%	1.44%	1.86%	1.00%
7 pm–10 pm	86.1%	0.92%	14.72%	1.41%	9.24%	0.63%	2.49%	0.14%	0.64%	3.37%	6.09%	1.29%	2.20%	0.95%	1.86%
10 pm–5 am	96.8%	1.84%	4.60%	0.00%	1.41%	0.04%	0.63%	0.03%	0.14%	0.62%	3.37%	0.08%	1.29%	0.20%	0.95%

**Table A13**  
Activity profile for “Jobless”.

Jobless Time	Home	To Shopping	From Shopping	To Private	From Private	To Leisure Res	From Leisure Res	To Leisure Genrl	From Leisure Genrl	To Leisure Sport	From Leisure Sport	To Leisure OutG	From Leisure OutG
5 am–8 am	98.2%	1.19%	0.77%	0.17%	0.10%	0.00%	0.00%	0.00%	0.09%	0.10%	0.00%	0.00%	0.04%
8 am–10 am	87.7%	7.92%	1.19%	1.12%	0.17%	0.47%	0.00%	0.23%	0.00%	0.89%	0.10%	0.11%	0.00%
10 am–1 pm	81.6%	10.92%	7.92%	2.12%	1.12%	1.10%	0.47%	0.66%	0.23%	1.09%	0.89%	0.31%	0.11%
1 pm–4 pm	83.2%	8.06%	10.92%	1.79%	2.12%	1.88%	1.10%	1.22%	0.66%	0.55%	1.09%	0.58%	0.31%
4 pm–7 pm	85.5%	5.38%	8.06%	2.11%	1.79%	1.41%	1.88%	1.74%	1.22%	0.51%	0.55%	0.82%	0.58%
7 pm–10 pm	95.8%	1.00%	5.38%	0.77%	2.11%	0.37%	1.41%	0.75%	1.74%	0.27%	0.51%	0.35%	0.82%
10 pm–5 am	98.9%	0.77%	1.00%	0.10%	0.77%	0.00%	0.37%	0.09%	0.75%	0.00%	0.27%	0.04%	0.35%

**Table A14**  
Activity profile for “Retired”.

Retired Time	Home	To Shopping	From Shopping	To Private	From Private	To Leisure Res	From Leisure Res	To Leisure Genrl	From Leisure Genrl	To Leisure Sport	From Leisure Sport	To Leisure OutG	From Leisure OutG
5 am–8 am	98.4%	0.82%	0.00%	0.23%	0.01%	0.08%	0.06%	0.03%	0.09%	0.16%	0.00%	0.00%	0.02%
8 am–10 am	89.9%	5.39%	0.82%	1.79%	0.23%	0.57%	0.08%	0.42%	0.03%	0.93%	0.16%	0.07%	0.00%
10 am–1 pm	78.6%	11.16%	5.39%	3.68%	1.79%	1.88%	0.57%	1.02%	0.42%	1.06%	0.93%	0.62%	0.07%
1 pm–4 pm	85.1%	5.60%	11.16%	1.80%	3.68%	2.26%	1.88%	1.30%	1.02%	0.85%	1.06%	0.42%	0.62%
4 pm–7 pm	89.1%	2.69%	5.60%	1.18%	1.80%	1.68%	2.26%	1.25%	1.30%	0.77%	0.85%	0.76%	0.42%
7 pm–10 pm	97.3%	0.29%	2.69%	0.15%	1.18%	0.44%	1.68%	0.72%	1.25%	0.24%	0.77%	0.33%	0.76%
10 pm–5 am	99.6%	0.00%	0.29%	0.01%	0.15%	0.06%	0.44%	0.09%	0.72%	0.00%	0.24%	0.02%	0.33%

**Table A15**  
Distance profile for the activity “Education”.

Education Time	to 0.36 km	to 0.72 km	to 1.44 km	to 3.6 km	to 7.2 km	to 14.4 km	to 36 km	to 72 km	over 72
5 am–8 am	4%	10%	15%	23%	22%	18%	7%	1%	0%
8 am–10 am	8%	9%	14%	23%	17%	14%	12%	3%	0%
10 am–1 pm	7%	15%	16%	23%	13%	13%	10%	2%	1%
1 pm–4 pm	10%	15%	23%	20%	13%	7%	11%	1%	0%
4 pm–7 pm	7%	6%	14%	17%	32%	10%	7%	4%	3%
7 pm–10 pm	7%	6%	14%	17%	32%	10%	7%	4%	3%
10 pm–5 am	7%	6%	14%	17%	32%	10%	7%	4%	3%

**Table A16**  
Distance profile for the activity “Work”.

Work Time	to 0.36 km	to 0.72 km	to 1.44 km	to 3.6 km	to 7.2 km	to 14.4 km	to 36 km	to 72 km	over 72
5 am–8 am	3%	5%	7%	16%	20%	24%	21%	4%	0%
8 am–10 am	4%	6%	8%	19%	20%	20%	18%	4%	1%
10 am–1 pm	7%	8%	11%	22%	21%	15%	11%	3%	2%
1 pm–4 pm	7%	10%	12%	20%	19%	18%	11%	2%	1%
4 pm–7 pm	6%	7%	10%	17%	19%	20%	14%	3%	4%
7 pm–10 pm	4%	3%	6%	12%	20%	22%	24%	6%	3%
10 pm–5 am	2%	6%	7%	19%	22%	20%	21%	2%	1%

**Table A17**  
Distance profile for the activity “Shopping”.

Shopping Time	To 0.36 km	To 0.72 km	To 1.44 km	To 3.6 km	To 7.2 km	To 14.4 km	To 36 km	To 72 km	Over 72
5 am–8 am	20%	26%	19%	22%	8%	3%	1%	0%	1%
8 am–10 am	15%	21%	21%	23%	14%	5%	1%	0%	0%
10 am–1 pm	14%	19%	19%	25%	13%	7%	3%	0%	0%
1 pm–4 pm	12%	17%	17%	24%	16%	9%	4%	1%	0%
4 pm–7 pm	15%	19%	17%	24%	13%	8%	3%	1%	0%
7 pm–10 pm	19%	23%	22%	18%	11%	5%	2%	0%	0%
10 pm–5 am	19%	23%	22%	18%	11%	5%	2%	0%	0%

**Table A18**  
Distance profile for the activity “Private”.

Private Time	to 0.36 km	to 0.72 km	to 1.44 km	to 3.6 km	to 7.2 km	to 14.4 km	to 36 km	to 72 km	over 72
5 am–8 am	11%	16%	20%	23%	14%	10%	4%	2%	0%
8 am–10 am	9%	12%	16%	26%	16%	12%	7%	1%	1%
10 am–1 pm	9%	12%	15%	24%	18%	12%	7%	2%	1%
1 pm–4 pm	8%	12%	14%	25%	17%	13%	8%	2%	1%
4 pm–7 pm	8%	13%	16%	23%	17%	12%	8%	2%	1%
7 pm–10 pm	8%	12%	17%	25%	14%	13%	7%	2%	2%
10 pm–5 am	8%	12%	14%	20%	11%	16%	9%	5%	5%

**Table A19**  
Distance profile for the activity “Leisure”.

Leisure Time	To 0.36 km	To 0.72 km	To 1.44 km	To 3.6 km	To 7.2 km	To 14.4 km	To 36 km	To 72 km	Over 72
5 am–8 am	5%	12%	24%	32%	13%	8%	3%	1%	2%
8 am–10 am	5%	10%	15%	32%	17%	11%	6%	3%	1%
10 am–1 pm	4%	8%	12%	27%	18%	12%	10%	5%	4%
1 pm–4 pm	5%	8%	13%	28%	17%	14%	9%	3%	3%
4 pm–7 pm	5%	10%	13%	29%	18%	12%	7%	3%	3%
7 pm–10 pm	6%	12%	16%	27%	17%	11%	7%	2%	2%
10 pm–5 am	5%	15%	14%	25%	11%	11%	11%	3%	5%

**Table A20**  
ALKIS building categories and with assigned building types.

ALKIS category	ALKIS category identifier	Type
Kinderkrippe_Kindergarten_Kindertagesstaette	3065	Day_Care100
Gebaeude_zur_Freizeitgestaltung	1310	Leisure_Genrl
Gartenhaus	1313	Leisure_Genrl
Huette_mit_uebernachtungsmoeglichkeit	2073	Leisure_Genrl
Huette_ohne_uebernachtungsmoeglichkeit	2082	Leisure_Genrl
Freizeit_und_Vergnuegungsstaette	2090	Leisure_Genrl
Kino	2092	Leisure_Genrl
Kegel_Bowlinghalle	2093	Leisure_Genrl
Reithalle	2728	Leisure_Genrl
Almhuetten	2732	Leisure_Genrl
Gebaeude_fuer_kulturelle_Zwecke	3030	Leisure_Genrl
Theater_Oper	3032	Leisure_Genrl
Konzertgebaeude	3033	Leisure_Genrl
Museum	3034	Leisure_Genrl
Veranstaltungsgebaeude	3036	Leisure_Genrl
Gemeindehaus	3044	Leisure_Genrl
Freizeit_Vereinsheim_Dorfgemeinschafts_Buergerhaus	3062	Leisure_Genrl
Gebaeude_fuer_Erholungszwecke	3200	Leisure_Genrl
Gebaeude_im_Zoo	3260	Leisure_Genrl
Aquarium_Terrarium_Voliere	3262	Leisure_Genrl
Tierschauhaus	3263	Leisure_Genrl
Gebaeude_im_botanischen_Garten	3270	Leisure_Genrl
Pflanzenschauhaus	3273	Leisure_Genrl
Gebaeude_fuer_andere_Erholungseinrichtung	3280	Leisure_Genrl
Gebaeude_fuer_Bewirtung	2080	Leisure_OutG
Gaststaette_Restaurant	2081	Leisure_OutG
Festsaal	2091	Leisure_OutG
Spielkasino	2094	Leisure_OutG
Spielhalle	2095	Leisure_OutG
Gebaeude_fuer_Sportzwecke	3210	Leisure_Sport
Gebaeude_zum_Sportplatz	3212	Leisure_Sport
Badegebaeude	3220	Leisure_Sport
Hallenbad	3221	Leisure_Sport
Wohngebaeude_mit_Gemeinbedarf	1110	n
Ferienhaus	1311	n
Wochenendhaus	1312	n
Sonstiges_Gebaeude_fuer_Gewerbe_und_Industrie	2200	n
Betriebsgebaeude_zu_Verkehrsanlagen_allgemein	2400	n
Betriebsgebaeude_fuer_Strassenverkehr	2410	n
Wartehalle	2412	n
Stellwerk_Blockstelle	2423	n
Flugzeughalle	2431	n
Werft_Halle	2441	n
Dock_Halle	2442	n
Bootshaus	2444	n
Betriebsgebaeude_zur_Seilbahn	2450	n
Spannwerk_zur_Drahtseilbahn	2451	n
Gebaeude_zum_Parken	2460	n
Parkhaus	2461	n
Parkdeck	2462	n
Garage	2463	n
Tiefgarage	2465	n
Wasserbehaelter	2513	n
Umspannwerk	2522	n
Umformer	2523	n
Reaktorgebaeude	2527	n
Turbinenhaus	2528	n
Kesselhaus	2529	n
Gaswerk	2571	n

(continued on next page)

Table A20 (continued)

ALKIS category	ALKIS category identifier	Type
Heizwerk	2580	n
Gebaeude_der_Klaeranlage	2611	n
Toilette	2612	n
Gebaeude_zur_Abfallbehandlung	2620	n
Muellbunker	2621	n
Gebaeude_zur_Muellverbrennung	2622	n
Gebaeude_der_Abfalldeponie	2623	n
Scheune	2721	n
Schuppen	2723	n
Stall	2724	n
Scheune_und_Stall	2726	n
Stall_fuer_Tiergrosshaltung	2727	n
Jagdhaus_Jagdhuette	2735	n
Treibhaus_Gewaechshaus	2740	n
Treibhaus	2741	n
Gewaechshaus_verschiebbar	2742	n
Schloss	3031	n
Burg_Festung	3038	n
Gebaeude_fuer_religioese_Zwecke	3040	n
Kirche	3041	n
Synagoge	3042	n
Kapelle	3043	n
Gotteshaus	3045	n
Moschee	3046	n
Tempel	3047	n
Kloster	3048	n
Schutzbunker	3074	n
Friedhofsgebaeude	3080	n
Trauerhalle	3081	n
Gebaeude_zum_UBahnhof	3094	n
Gebaeude_zum_SBahnhof	3095	n
Gebaeude_zum_Busbahnhof	3097	n
Empfangsgebaeude_Schiffahrt	3098	n
Schutzhuette	3281	n
Nach_Quellenlage_nicht_zu_spezifizieren	9998	n
Tankstelle	2130	Private100
Waschstrasse_Waschanlage_Waschhalle	2131	Private100
Schwesterwohnheim	1023	Residential10
Land_und_forstwirtschaftliches_Wohngebaeude	1210	Residential10
Campingplatzgebaeude	2074	Residential10
Wohn_und_Wirtschaftsgebaeude	1222	Residential10_Work25
Gebaeude_fuer_Handel_und_Dienstleistung_mit_Wohnen	2310	Residential10_Work25
Gebaeude_fuer_Gewerbe_und_Industrie_mit_Wohnen	2320	Residential10_Work25
Asylbewerberheim	3066	Residential100
Justizvollzugsanstalt	3075	Residential100_Work25
Wohn_und_Betriebsgebaeude	1131	Residential20_Work25
Heilanstalt_Pflegeanstalt_Pflegestation	3052	Residential20_Work25
Bauernhaus	1221	Residential30
Forsthaus	1223	Residential30
Wohn_und_Buerogebaeude	1122	Residential30_Work25
Land_und_forstwirtschaftliches_Wohn_und_Betriebsgebaeude	1220	Residential30_Work25
Wohnheim	1020	Residential40
Seniorenheim	1022	Residential40
Schullandheim	1025	Residential40
Gemischt_genutztes_Gebaeude_mit_Wohnen	1100	Residential40
Jugendfreizeitheim	3061	Residential40
Obdachlosenheim	3064	Residential40
Gebaeude_fuer_soziale_Zwecke	3060	Residential40_Work12.5
Gebaeude_fuer_oeffentliche_Zwecke_mit_Wohnen	3100	Residential40_Work25
Gebaeude_fuer_Beherbergung	2070	Residential50
Hotel_Motel_Pension	2071	Residential50
Jugendherberge	2072	Residential50
Seniorenfreizeitstaette	3063	Residential50_Work10
Sanatorium	3242	Residential50_Work10
Wohngebaeude_mit_Handel_und_Dienstleistungen	1120	Residential50_Work12.5
Wohn_und_Geschaeftsgebaeude	1123	Residential50_Work12.5
Wohn_und_Verwaltungsgebaeude	1121	Residential50_Work25
Wohngebaeude_mit_Gewerbe_und_Industrie	1130	Residential50_Work25
Rettungswache	3054	Residential50_Work25
Polizei	3071	Residential50_Work25
Feuerwehr	3072	Residential50_Work25
Kaserne	3073	Residential50_Work25
Gebaeude_fuer_Kurbetrieb	3240	Residential50_Work25
Wohngebaeude	1000	Residential70
Wohnhaus	1010	Residential70
Kinderheim	1021	Residential70

(continued on next page)

Table A20 (continued)

ALKIS category	ALKIS category identifier	Type
Studenten_Schuelerwohnheim	1024	Residential90
Allgemein_bildende_Schule	3021	School
Berufsbildende_Schule	3022	School
Sport_Turnhalle	3211	School
Kaufhaus	2051	Shopping100
Einkaufszentrum	2052	Shopping100
Markthalle	2053	Shopping100
Laden	2054	Shopping100
Kiosk	2055	Shopping100
Gebaeude_fuer_Bildung_und_Forschung	3020	University
Hochschulgebaeude_Fachhochschule_Universityversitaet	3023	University
Buerogebaeude	2020	Work100
Kantine	2083	Work12.5
Gebaeude_fuer_Gewerbe_und_Industrie	2100	Work12.5
Fabrik	2111	Work12.5
Saegewerk	2121	Work12.5
Gebaeude_fuer_Forschungszwecke	2160	Work12.5
Strassenmeisterei	2411	Work12.5
Bahnwaerterhaus	2421	Work12.5
Betriebsgebaeude_des_Gueterbahnhofs	2424	Work12.5
Betriebsgebaeude_fuer_Schiffsverkehr	2440	Work12.5
Betriebsgebaeude_zur_Schleuse	2443	Work12.5
Land_und_forstwirtschaftliches_Betriebsgebaeude	2720	Work12.5
Wirtschaftsgebaeude	2729	Work12.5
Krematorium	3082	Work12.5
Empfangsgebaeude	3090	Work12.5
Bahnhofsgebaeude	3091	Work12.5
Flughafengebaeude	3092	Work12.5
Touristisches_Informationszentrum	3290	Work12.5
Bibliothek_Buecherei	3037	Work12.5_Private25
Apotheke	2056	Work12.5_Private75
Gebaeude_fuer_oeffentliche_Zwecke	3000	Work12.5_Private75
Post	3013	Work12.5_Private75
Gebaeude_fuer_Gesundheitswesen	3050	Work12.5_Private75
aerztheus_Poliklinik	3053	Work12.5_Private75
Speichergebaeude	2142	Work2.5
Lokschuppen_Wagenhalle	2422	Work2.5
Fahrzeughalle	2464	Work2.5
Wasserwerk	2511	Work2.5
Pumpstation	2512	Work2.5
Elektrizitaetswerk	2521	Work2.5
Gebaeude_an_unterirdischen_Leitungen	2560	Work2.5
Gebaeude_zur_Gasversorgung	2570	Work2.5
Gebaeude_zur_Versorgungsanlage	2590	Work2.5
Pumpwerk_nicht_fuer_Wasserversorgung	2591	Work2.5
Gebaeude_zur_Abwasserbeseitigung	2610	Work2.5
Gebaeude_fuer_Land_und_Forstwirtschaft	2700	Work2.5
Gebaeude_im_Freibad	3222	Work2.5
Gebaeude_im_Stadion	3230	Work2.5
Stall_im_Zoo	3264	Work2.5
Gewaechshaus_Botanik	3272	Work2.5
Betriebsgebaeude	2112	Work25
Brauerei	2113	Work25
Brennerei	2114	Work25
Werkstatt	2120	Work25
Gebaeude_zur_Entsorgung	2600	Work25
Gebaeude_fuer_betriebliche_Sozialeinrichtung	2180	Work25_Private50
Produktionsgebaeude	2110	Work37.5
Messehalle	2060	Work5
Gebaeude_fuer_Vorratshaltung	2140	Work5
Kuehlhaus	2141	Work5
Lagerhalle_Lagerschuppen_Lagerhaus	2143	Work5
Gebaeude_fuer_Grundstoffgewinnung	2170	Work5
Bergwerk	2171	Work5
Saline	2172	Work5
Muehle	2210	Work5
Windmuehle	2211	Work5
Wassermuehle	2212	Work5
Schoepfwerk	2213	Work5
Wetterstation	2220	Work5
Betriebsgebaeude_fuer_Schienenverkehr	2420	Work5
Betriebsgebaeude_fuer_Flugverkehr	2430	Work5
Gebaeude_zur_Versorgung	2500	Work5
Gebaeude_zur_Energieversorgung	2501	Work5
Gebaeude_zur_Wasserversorgung	2510	Work5
Gebaeude_zur_Elektrizitaetsversorgung	2520	Work5

(continued on next page)

**Table A20 (continued)**

ALKIS category	ALKIS category identifier	Type
Gebaeude_fuer_Fernmeldewesen	2540	Work5
Empfangsgebaeude_des_Zoos	3261	Work5
Empfangsgebaeude_des_botanischen_Gartens	3271	Work5
Gebaeude_fuer_Wirtschaft_oder_Gewerbe	2000	Work50
Parlament	3011	Work50
Rathaus	3012	Work50
Zollamt	3014	Work50
Botschaft_Konsulat	3016	Work50
Gebaeude_fuer_Sicherheit_und_Ordnung	3070	Work50
Gericht	3015	Work50_Private50
Krankenhaus	3051	Work50_Private50
Badegebaeude_fuer_medizinische_Zwecke	3241	Work50_Private50
Gebaeude_fuer_Handel_und_Dienstleistungen	2010	Work62.5
Geschaeftsgebaeude	2050	Work62.5
Forschungsinstitut	3024	Work62.5
Speditionsgebaeude	2150	Work7.5
Kreisverwaltung	3017	Work75
Bezirksregierung	3018	Work75
Rundfunk_Fernsehen	3035	Work75
Verwaltungsgebaeude	3010	Work87.5
Finanzamt	3019	Work87.5
Kreditinstitut	2030	Work87.5_Private25
Versicherung	2040	Work87.5_Private25

**Appendix B. Formulas**

*Calculating the distribution variables*

The activity-dependent distribution variable ( $v$ ) of a building ( $b$ ) is calculated individually for each activity. A building can serve as an execution location for up to two activities and thus be assigned two distribution variables.  $v$  is calculated from the product of the building floor area ( $A$ ) and height ( $h$ ), as well as the weighting ( $w$ ), which, depending on the building type ( $y$ ), represents a density of people in the building to be expected for the respective activity ( $a$ ).

$$v_{b,y,a} = A_b * h_b * w_{y,a}$$

*Calculation of time-dependent population per hexagon*

Basically, the model calculates the population entering and leaving per time interval for each hexagon on the one hand, and calculates directly for the surrounding hexagons how many people entering and leaving these movements lead to. So a departing person is subtracted once at the start hexagon and added to the target hexagon (or vice versa), and thus appears twice in the calculation.

The total population ( $P_{total}$ ) of a hexagon ( $H$ ) at a given time ( $t$ ) consists of the people who stay at home ( $P_{home,t,H}$ ) and the people who leave the hexagon  $H$  ( $P_{out,t,H}$ ) and the ones who come into  $H$  ( $P_{in,t,H}$ ). These, in turn, are composed of the respective sum of the persons of all seven subgroups ( $g$ ).

$$P_{total,t,H} = P_{home,t,H} + P_{in,t,H} - P_{out,t,H}$$

$$P_{home,t,H} = \sum P_{home,g,t,H}$$

$$P_{in,t,H} = \sum P_{in,g,t,H}$$

$$P_{out,t,H} = \sum P_{out,g,t,H}$$

The base population ( $P_{base,H}$ ) is the population living in Hexagon  $H$  and is derived from the base residence dataset (Chapter 2.2 “Base residence dataset”). People from  $P_{base,H}$  stay either at home, leave  $H$  for an activity or arrive back home from an activity ( $a$ ).  $P_{base,H}$  serves as the basis for calculating the mobility behavior of  $H$ .

$P_{home,H}$  is the share  $s_{home}$  of  $P_{base,H}$  that stays at home in the time interval  $t$ . The time interval  $t$  and subgroup  $g$  dependent shares are taken from [Tables A8–A14 in Appendix A](#).

$$P_{home,g,t,H} = P_{base,g,H} * s_{home,g}$$

The incoming  $P_{in,g,t,H}$  and outgoing population  $P_{out,g,t,H}$  consists of each two groups.  $P_{in,g,t,H}$  is composed of the people living in  $H$  who return from an activity from an external hexagon ( $P_{int-in,g,t,H}$ ) as well as the people from an external hexagon who come to the  $H$  for an activity  $a$  ( $P_{ext-in,g,t,H}$ ).  $P_{out,g,t,H}$  is composed of the people living in  $H$  who leave  $H$  for an activity  $a$  ( $P_{int-out,g,t,H}$ ) as well as the external people who return from  $H$  to their external home hexagon after an activity ( $P_{ext-out,g,t,H}$ ).

$$P_{in,g,t,H} = P_{int-in,g,t,H} + P_{ext-in,g,t,H}$$

$$P_{out,g,t,H} = P_{int-out,g,t,H} + P_{ext-out,g,t,H}$$

$P_{int-out,g,t,H}$  and  $P_{int-in,g,t,H}$  consist of the sum of the internal people who leave or return from  $H$  for one of the seven activities. This group is described by the respective share  $s$  (dependent on  $t$ ,  $g$ , and  $a$ ) of the population  $P_{base,H}$  residing in  $H$ , which can be taken from [Tables A8–A14 of Appendix A](#). Where  $s_{to,a,g,t}$  describes the proportion that goes to an activity, while  $s_{from,a,g,t}$  describes the proportion that comes back.

$$P_{int-out,g,t,H} = \sum P_{int-out,a,g,t,H}$$

$$P_{int-out,a,g,t,H} = P_{base,g,H} * S_{to,a,g,t}$$

$$P_{int-in,g,t,H} = \sum_a P_{int-in,a,g,t,H}$$

$$P_{int-in,a,g,t,H} = P_{base,g,H} * S_{from,a,g,t}$$

$P_{int-out,a,g,t,H}$  describes the part of the subgroup  $g$  living in hexagon  $H$  that leaves  $H$  in the time interval  $t$  to a specific activity  $a$ . These people are specifically distributed to surrounding hexagons based on their mobility characteristics and the building characteristics of the surrounding urban area. For each variation of these groups of people, the following dasymetric population distribution process is carried out (Chapter 2.3.2 “Activity informed population distribution”). To determine where people travel for their activity,  $P_{int-out,a,g,t,H}$  is further divided based on the average travel distance expressed as proportion ( $k$ ) per activity (Tables A15–A19 in Appendix A).  $P_{int-out,d,a,g,t,H}$  thus indicates the number of people of a subgroup  $g$  from a hexagon  $H$  who travel a certain distance  $d$  at a certain time  $t$ , for a certain activity  $a$ .

$$P_{int-out,d,a,g,t,H} = P_{int-out,a,g,t,H} * k_{d,a,t}$$

To assign  $P_{int-out,d,a,g,t,H}$  to the hexagons at the respective distance (corresponding to  $k$ ), all hexagons that are at a distance  $d$  from hexagon  $H$  are selected ( $H_d$ ). The distribution of  $P_{int-out,d,a,g,t,H}$  on these is based on the share of the respective distribution variable ( $v$ ) in the sum of  $v$  of all  $H_d$ .  $v$  of a hexagon is the sum of all  $v$  of the buildings ( $b$ ) of the hexagon.

$$v_{H,a} = \sum_{b_H} v_{a,b}$$

This assigns a proportion ( $P_x$ ) of  $P_{int-out,d,a,g,t,H}$  to each hexagon ( $H_i$ ) of group  $H_d$  for each distance calculation step  $d$ , based on the buildings that occur in the respective hexagon.

$$P_{x,H_i} = P_{int-out,d,a,g,t,H} * \frac{v_{H_i,a}}{\sum_{H_d} v_{H_d,a}}$$

In order to obtain  $P_{ext-in,g,t,H}$  meaning the people who enter  $H$  from an external hexagon to carry out an activity there, all  $P_x$  which are assigned to  $H$  during the calculation of the  $P_{int-out,d,a,g,t,H}$  value of respective external hexagons ( $P_{x,H}$ ) are summed up.

$$P_{ext-in,g,t,H} = \sum P_{x,H}$$

Analogous to the previously described distribution process of  $P_{int-out,a,g,t,H}$   $P_{int-in,a,g,t,H}$  is used to calculate how many people ( $P_y$ ) are subtracted from the surrounding hexagons ( $H_d$ ) because they return to  $H$ .  $P_y$  embodies the reduction in  $H_d$  initiated by people that leave the surrounding hexagons to which they have previously traveled.

$$P_{int-in,d,a,g,t,H} = P_{int-in,a,g,t,H} * k_{d,a,t}$$

$$P_{y,H_i} = P_{int-in,d,a,g,t,H} * \frac{v_{H_i,a}}{\sum_{H_d} v_{H_d,a}}$$

In order to obtain  $P_{ext-out,g,t,H}$ , meaning the people who leave  $H$ , to return home after they finished their activity in  $H$ , all  $P_y$  which have been assigned to  $H$  during the calculation of the  $P_{int-in,d,a,g,t,H}$  value of respective external hexagons ( $P_{x,H}$ ) are summed up.

$$P_{ext-out,g,t,H} = \sum P_{y,H}$$

## Data availability

R-Code and Results are available via the Mandalay Data Repository: [Modelling spatio-temporal distribution of urban population - A high-resolution model for German cities \(Original data\)](#) (Mendeley Data)

## References

Ahola, T., Verrantaus, K., Krisp, J. M., & Hunter, G. J. (2007). A spatio-temporal population model to support risk assessment and damage analysis for decision-making. *International Journal of Geographical Information Science*, 21(8), 935–953. <https://doi.org/10.1080/13658810701349078>

Aubrecht, C. (2013a). *A geospatial perspective on population exposure and social vulnerability in disaster risk research*. Dissertation. Technische Universität Wien. <https://doi.org/10.34726/hss.2013.1271>. Available online at reposiTUM.

Aubrecht, C. (2013b). *A geospatial perspective on population exposure and social vulnerability in disaster risk research: Demonstrating the importance of spatial and temporal scale and thematic context*. TU Wien.

Aubrecht, C., Steinnocher, K., & Huber, H. (2014). DynaPop – population distribution dynamics as basis for social impact evaluation in crisis management. In *ISCRAM 2014 conference proceedings 11th international conference on information systems for crisis response and management*.

Aubrecht, C., Steinnocher, K., Kostl, M., & Grisel, M. (2015). Dynamic population exposure modeling: Application of DynaPop-X for storm surge related coastal flood crisis management. In *2015 IEEE international geoscience and remote sensing symposium*. <https://doi.org/10.1109/IGARSS.2015.7326333>. Milan, Italy.

Batista E Silva, F., Freire, S., Schiavina, M., Rosina, K., Marín-Herrera, M. A., Ziemba, L., et al. (2020). Uncovering temporal changes in Europe’s population density patterns using a data fusion approach. *Nature Communications*, 11(1), Article 4631. <https://doi.org/10.1038/s41467-020-18344-5>

Behrens, J., Løvholt, F., Jalayer, F., Lorito, S., Salgado-Gálvez, M. A., Sørensen, M., et al. (2021). Probabilistic tsunami hazard and risk analysis: A review of research gaps. *Frontiers in Earth Science*, 9, Article 628772. <https://doi.org/10.3389/feart.2021.628772>

Bengtsson, L., Lu, X., Thorson, A., Garfield, R., & von Schreeb, J. (2011). Improved response to disasters and outbreaks by tracking population movements with mobile phone network data: A post-earthquake geospatial study in Haiti. *PLoS Medicine*, 8(8), Article e1001083. <https://doi.org/10.1371/journal.pmed.1001083>

Birch, C. P. D., Oom, S. P., & Beecham, J. A. (2007). Rectangular and hexagonal grids used for observation, experiment and simulation in ecology. *Ecological Modelling*, 206(3–4), 347–359. <https://doi.org/10.1016/j.ecolmodel.2007.03.041>

- Cats, O. (2024). Identifying human mobility patterns using smart card data. *Transport Reviews*, 44(1), 213–243. <https://doi.org/10.1080/01441647.2023.2251688>
- Chen, J., Pei, T., Li, M., Song, C., Ma, T., Lu, F., & Shaw, S.-L. (2020). An enhanced model for evacuation vulnerability assessment in urban areas. *Computers, Environment and Urban Systems*, 84, Article 101540. <https://doi.org/10.1016/j.compenurbysys.2020.101540>
- City of Cologne. (2018). Kölner Statistische Nachrichten 4/2018. Erwerbstätigkeit und wirtschaftliche Lage der Kölner Bevölkerung. Ergebnisse der "Leben in Köln"-Umfrage 2016. Available online at [https://www.stadt-koeln.de/mediaasset/content/pdf15/statistik-umfragen/erwerbst%C3%A4tigkeit\\_und\\_wirtschaftliche\\_lage\\_der\\_k%C3%B6lnerbev%C3%B6lkerung\\_um\\_ksn\\_2018\\_4.pdf](https://www.stadt-koeln.de/mediaasset/content/pdf15/statistik-umfragen/erwerbst%C3%A4tigkeit_und_wirtschaftliche_lage_der_k%C3%B6lnerbev%C3%B6lkerung_um_ksn_2018_4.pdf) (checked on 5/22/2024).
- City of Cologne. (2022). Kindertagesstätten in Koeln. Edited by Offene Daten Köln. Available online at <https://www.offenedaten-koeln.de/dataset/kindertagesstaetten-koeln> (updated on 8/10/2022, checked on 5/23/2025).
- City of Cologne. (2024a). Statistisches Jahrbuch 2023. Kölner Statistische Nachrichten 9/2024. Kapitel 1: Bevölkerung und Haushalte. Available online at [https://www.stadt-koeln.de/mediaasset/content/pdf15/statistik-jahrbuch/ksn\\_9\\_2024\\_statistisches\\_jahrbuch\\_2023.pdf](https://www.stadt-koeln.de/mediaasset/content/pdf15/statistik-jahrbuch/ksn_9_2024_statistisches_jahrbuch_2023.pdf) (checked on 5/22/2024).
- City of Cologne. (2024b). Statistisches Jahrbuch 2023. Kölner Statistische Nachrichten 9/2024. Kapitel 6: Bildung und Ausbildung. Available online at [https://www.stadt-koeln.de/mediaasset/content/pdf15/statistik-jahrbuch/ksn\\_9\\_2024\\_statistisches\\_jahrbuch\\_2023.pdf](https://www.stadt-koeln.de/mediaasset/content/pdf15/statistik-jahrbuch/ksn_9_2024_statistisches_jahrbuch_2023.pdf) (checked on 5/22/2024).
- City of Cologne. (2024c). Statistischer Datenkatalog Köln. Edited by Offene Daten Köln. Available online at <https://offenedaten-koeln.de/dataset/statistischer-datenkatalog-k%C3%B6ln> (updated on 9/19/2024, checked on 5/22/2025).
- Cockings, S., Martin, D., Harfoot, A., Branson, J., Campbell-Sutton, A., & Gubbins, G. (2021). *Population 24/7 near real time: Data library, sample outputs and batch files for England, 2011*.
- Cologne District Government. (2025). ALKIS-Standard. Edited by Bezirksregierung Köln. Available online at <https://www.bezreg-koeln.nrw.de/geobasis-nrw/produkte-und-dienste/liegenschaftskataster/alkis-standard> (checked on 5/21/2025).
- Cui, P., Peng, J., Shi, P., Tang, H., Ouyang, C., Zou, Q., et al. (2021). Scientific challenges of research on natural hazards and disaster risk. *Geography and Sustainability*, 2(3), 216–223. <https://doi.org/10.1016/j.geosus.2021.09.001>
- Cutter, S. L., Mitchell, J. T., & Scott, M. S. (2000). Revealing the vulnerability of people and places: A case study of Georgetown County, South Carolina. *Annals of the Association of American Geographers*, 90(4), 713–737. <https://doi.org/10.1111/0004-5608.00219>
- Deville, P., Linaud, C., Martin, S., Gilbert, M., Stevens, F. R., Gaughan, A. E., et al. (2014). Dynamic population mapping using mobile phone data. *Proceedings of the National Academy of Sciences of the United States of America*, 111(45), 15888–15893. <https://doi.org/10.1073/pnas.1408439111>
- Doyle, J., Hung, P., Farrell, R., & McLoone, S. (2014). Population mobility dynamics estimated from mobile telephony data. *Journal of Urban Technology*, 21(2), 109–132. <https://doi.org/10.1080/10630732.2014.888904>
- European Commission. (2025). *INSPIRE Geoportall. Enabling access to European geospatial data for the Green Deal*. European Commission Joint Research Centre. Available online at <https://inspire-geoportall.ec.europa.eu> (updated on 5/22/2025, checked on 5/22/2025).
- Federal Employment Agency of Germany. (2024). In Bundesagentur für Arbeit Statistik (Ed.), *Strukturdaten der Agentur für Arbeit Köln. Kurzübersicht*. Available online at <http://www.arbeitsagentur.de/vor-ort/koeln/statistik> (checked on 5/22/2025).
- Federal Statistical Office of Germany. (2023). In Destatis (Ed.), *Erwerbstätigkeit älterer Menschen*. Available online at [https://www.destatis.de/DE/Themen/Querschnitt/De\\_mografischer\\_Wandel/Aeltere-Menschen/erwerbstaeftigkeit.html;jsessionid=28CAC26DE7C95D062F8E6BB1CE14CD51.live?731](https://www.destatis.de/DE/Themen/Querschnitt/De_mografischer_Wandel/Aeltere-Menschen/erwerbstaeftigkeit.html;jsessionid=28CAC26DE7C95D062F8E6BB1CE14CD51.live?731) (checked on 5/22/2025).
- Federal Statistical Office of Germany. (2024). *59% der 18- bis 24-Jährigen sind in Schule, Ausbildung oder Studium*. Wiesbaden: Destatis. Available online at [https://www.destatis.de/DE/Presse/Pressemitteilungen/2024/05/PD24\\_N021\\_12\\_63.html](https://www.destatis.de/DE/Presse/Pressemitteilungen/2024/05/PD24_N021_12_63.html) (updated on 5/22/2024, checked on 5/22/2025).
- Follmer, R. (2025). Mobilität in Deutschland - MiD Kurzbericht. In *Studie von infas, DLR, IVT und infas 360 im Auftrag des Bundesministers für Digitales und Verkehr (FE-Nr. VB600001)*. Bonn, Berlin. Available online at <https://www.mobilitaet-in-deutsche-land.de/>.
- Freire, S., & Aubrecht, C. (2012). Integrating population dynamics into mapping human exposure to seismic hazard. *Natural Hazards and Earth System Sciences*, 12(11), 3533–3543. <https://doi.org/10.5194/nhess-12-3533-2012>
- Freire, S. (2010). Modeling of spatiotemporal distribution of urban population at high resolution – Value for risk assessment and emergency management. *Geographic Information and Cartography for Risk and Crisis Management*, 53–67. [https://doi.org/10.1007/978-3-642-03442-8\\_4](https://doi.org/10.1007/978-3-642-03442-8_4)
- Freire, S., Aubrecht, C., & Wegscheider, S. (2013). Advancing tsunami risk assessment by improving spatio-temporal population exposure and evacuation modeling. *Natural Hazards*, 68(3), 1311–1324. <https://doi.org/10.1007/s11069-013-0603-4>
- Gao, Y., Janssen, M., & Zhang, C. (2023). Understanding the evolution of open government data research: Towards open data sustainability and smartness. *International Review of Administrative Sciences*, 89(1), 59–75. <https://doi.org/10.1177/00208523211009955>
- Gariazzo, C., Pelliccioni, A., & Bolognino, A. (2016). A dynamic urban air pollution population exposure assessment study using model and population density data derived by mobile phone traffic. *Atmospheric Environment*, 131, 289–300. <https://doi.org/10.1016/j.atmosenv.2016.02.011>
- GDI-DE. (2025). Spatial Data Infrastructure Germany. Edited by Geodateninfrastruktur Deutschland. Available online at <https://www.gdi-de.org/en> (updated on 5/22/2025, checked on 5/22/2025).
- Geiß, C., Maier, J., So, E., Schoepfer, E., Harig, S., Gómez Zapata, J. C., & Zhu, Y. (2024). Anticipating a risky future: Long short-term memory (LSTM) models for spatiotemporal extrapolation of population data in areas prone to earthquakes and tsunamis in Lima, Peru. *Natural Hazards and Earth System Sciences*, 24(3), 1051–1064. <https://doi.org/10.5194/nhess-24-1051-2024>
- Geiß, C., Priesmeier, P., Aravena Pelizari, P., Soto Calderon, A. R., Schoepfer, E., Riedlinger, T., et al. (2022). Benefits of global earth observation missions for disaggregation of exposure data and earthquake loss modeling: Evidence from Santiago de Chile. *Natural Hazards*, 119(2), 779–804. <https://doi.org/10.1007/s11069-022-05672-6>
- Gunkel, J., Mühlhäuser, M., & Tundis, A. (2025). Machine learning for human mobility during disasters: A systematic literature review. *In Progress in Disaster Science*, 25, Article 100405. <https://doi.org/10.1016/j.pdisas.2025.100405>
- Gunnhild, B. A. S., Tørset, T., & Lohne, J. (2024). A comparative study of national travel surveys in six European countries. *Transportation Planning and Technology*, 47(3), 400–418. <https://doi.org/10.1080/03081060.2024.2311081>
- Haberl, M., Fuchs, F., Winter, K., Streibl, M., & Cik, M. (2025). Mobilfunkdaten-gestützte Analyse des Mobilitätsverhaltens infolge extremer Wettersituationen. In *REAL CORP 2025 Proceedings/Tagungsband*. Available online at <https://www.corp.at/>
- Han, S. Y., Tsou, M.-H., Knaap, E., Rey, S., & Cao, G. (2019). How do cities flow in an emergency? Tracing human mobility patterns during a natural disaster with big data and geospatial data science. *Urban Science*, 3(2), 51. <https://doi.org/10.3390/urbansci3020051>
- Haraguchi, M., Nishino, A., Kodaka, A., Allaire, M., Lall, U., Kuei-Hsien, L., et al. (2022). Human mobility data and analysis for urban resilience: A systematic review. *Environment and Planning B: Urban Analytics and City Science*, 49(5), 1507–1535. <https://doi.org/10.1177/23998083221075634>
- Herfort, B., Lautenbach, S., Porto de Albuquerque, J., Anderson, J., & Zipf, A. (2023). A spatio-temporal analysis investigating completeness and inequalities of global urban building data in OpenStreetMap. *Nature Communications*, 14(1), Article 3985. <https://doi.org/10.1038/s41467-023-39698-6>
- IT.NRW. (2024a). *Pendleratlas Deutschland*. Edited by Information und Technik Nordrhein-Westfalen. Available online at <https://pendleratlas.statistikportal.de/> (updated on 10/15/2024, checked on 5/22/2025).
- IT.NRW. (2024b). *Qualitätsbericht. Pendlerrechnung der Länder*. Edited by Information und Technik Nordrhein-Westfalen. Available online at [https://www.statistikportal.de/sites/default/files/2024-10/Qualitaet%20C3%A4tsbericht\\_PendL\\_2024-10-16\\_0.pdf](https://www.statistikportal.de/sites/default/files/2024-10/Qualitaet%20C3%A4tsbericht_PendL_2024-10-16_0.pdf) (checked on 5/22/2025).
- Kroher, M., Beuße, M., Isleib, S., Becker, K., Erhardt, M. C., Gerdes, F., et al. (2023). The student survey in Germany: 22nd social survey. The economic and social situation of students in Germany 2021. (Edited by Federal Ministry for Education and Research. Available online at [https://www.dzhw.eu/pdf/ab\\_20/Soz22\\_Exec\\_Summary\\_en.pdf](https://www.dzhw.eu/pdf/ab_20/Soz22_Exec_Summary_en.pdf)
- Lebakula, V., Sims, K., Reith, A., Rose, A., McKee, J., Coleman, P., et al. (2025). LandScan global 30 arcsecond annual global gridded population datasets from 2000 to 2022. *Scientific Data*, 12(1). <https://doi.org/10.1038/s41597-025-04817-z>
- Leyk, S., Gaughan, A. E., Adamo, S. B., de Sherbinin, A., Balk, D., Freire, S., et al. (2019). The spatial allocation of population: A review of large-scale gridded population data products and their fitness for use. *Earth System Science Data*, 11(3), 1385–1409. <https://doi.org/10.5194/essd-11-1385-2019>
- Liu, K., Murayama, Y., & Ichinose, T. (2021). A multi-view of the daily urban rhythms of human mobility in the Tokyo metropolitan area. *Journal of Transport Geography*, 91, Article 102985. <https://doi.org/10.1016/j.jtrangeo.2021.102985>
- Liu, Z., Ma, T., Du, Y., Pei, T., Yi, J., & Peng, H. (2018). Mapping hourly dynamics of urban population using trajectories reconstructed from mobile phone records. *Transactions in GIS*, 22(2), 494–513. <https://doi.org/10.1111/tgis.12323>
- Ma, Y., Xu, W., Zhao, X., & Li, Y. (2017). Modeling the hourly distribution of population at a high spatiotemporal resolution using subway smart card data: A case study in the central area of Beijing. *International Journal of Geo-Information*, 6(5), Article 128. <https://doi.org/10.3390/ijgi6050128>
- Martin, D., Cockings, S., & Leung, S. (2009). *Population 24/7: Building time-specific population grid models*. In *European forum for geostatistics conference, The Hague, Netherlands (05–09 Oct 2009, 11 pp)*.
- Martin, D., Cockings, S., & Leung, S. (2015). Developing a flexible framework for spatiotemporal population modeling. *Annals of the Association of American Geographers*, 105(4), 754–772. <https://doi.org/10.1080/00045608.2015.1022089>
- Nobis, C., & Kuhnimhof, T. (2018). *Mobilität in Deutschland - MiD Ergebnisbericht*. Study of infas, DLR, IVT and infas 360 on behalf of the German Federal Ministry of Digital and Transport (FE-Nr. 70.904/15). Available online at [www.mobilitaet-in-deutschland.de](http://www.mobilitaet-in-deutschland.de).
- Openshaw, S. (1984). *The modifiable areal unit problem. Concepts and techniques in modern geography: Norwich (Geo Books, 38)*.
- OpenStreetMap Contributors. (2025). Download OpenStreetMap data for this region: Regierungsbezirk Köln. Edited by Geofabrik GmbH. Available online at <https://download.geofabrik.de/europe/germany/nordrhein-westfalen/koeln-regbez.html> (updated on 5/22/2025, checked on 5/23/2025).
- Pappalardo, L., Manley, E., Sekara, V., & Alessandretti, L. (2023). Future directions in human mobility science. *Nature Computational Science*, 3(7), 588–600. <https://doi.org/10.1038/s43588-023-00469-4>
- Pesaresi, M., Schiavina, M., Politis, P., Freire, S., Krasnodębska, K., Uhl, J. H., et al. (2024). Advances on the global human settlement layer by joint assessment of earth observation and population survey data. *International Journal of Digital Earth*, 17(1), Article 2390454. <https://doi.org/10.1080/17538947.2024.2390454>
- Pittore, M., Campalani, P., Renner, K., Plörner, M., & Tagliavini, F. (2023). Border-independent multi-functional, multi-hazard exposure modelling in Alpine regions. *Natural Hazards*, 119(2), 837–858. <https://doi.org/10.1007/s11069-023-06134-3>

- Pittore, M., Wieland, M., & Fleming, K. (2017). Perspectives on global dynamic exposure modelling for geo-risk assessment. *Natural Hazards*, 86(S1), 7–30. <https://doi.org/10.1007/s11069-016-2437-3>
- Qi, W., Liu, S., Gao, X., & Zhao, M. (2015). Modeling the spatial distribution of urban population during the daytime and at night based on land use: A case study in Beijing, China. *Journal of Geographical Sciences*, 25(6), 756–768. <https://doi.org/10.1007/s11442-015-1200-0>
- Rahimi-Golkhandan, A., Garvin, M. J., & Wang, Q. (2021). Assessing the impact of transportation diversity on postdisaster intraurban mobility. *Journal of Management in Engineering*, 37(1), Article 04020106. [https://doi.org/10.1061/\(ASCE\)JME.1943-5479.0000872](https://doi.org/10.1061/(ASCE)JME.1943-5479.0000872)
- Rauch, S., Taubenböck, H., Knopp, C., & Rauh, J. (2021). Risk and space: Modelling the accessibility of stroke centers using day- & nighttime population distribution and different transportation scenarios. *International Journal of Health Geographics*, 20(1), Article 31. <https://doi.org/10.1186/s12942-021-00284-y>
- Renner, K., Schneiderbauer, S., Pruiß, F., Köfler, C., Martin, D., & Cockings, S. (2018). Spatio-temporal population modelling as improved exposure information for risk assessments tested in the Autonomous Province of Bolzano. *International Journal of Disaster Risk Reduction*, 27, 470–479. <https://doi.org/10.1016/j.ijdrr.2017.11.011>
- Sapena, M., Kühnl, M., Wurm, M., Patino, J. E., Duque, J. C., & Taubenböck, H. (2022). Empiric recommendations for population disaggregation under different data scenarios. *PLoS One*, 17(9), Article e0274504. <https://doi.org/10.1371/journal.pone.0274504>
- Schiavina, M., Batista, F., Rosina, K., Ziemba, L., Marin Herrera, M., Craglia, M., et al. (2020). ENACT-POP R2020A - ENACT 2011 population grid.
- Schultz, M., Li, H., Wu, Z., Wiell, D., Auer, M., & Zipf, A. (2024). *OpenStreetMap land use for Europe “research data”* (With assistance of Michael Schultz).
- Sekara, V., Omodei, E., Healy, L., Beise, J., Hansen, C., You, D., et al. (2019). Mobile phone data for children on the move: Challenges and opportunities. In *Guide to mobile data analytics in refugee scenarios* (pp. 53–66). Cham: Springer. <https://doi.org/10.1007/978-3-030-12554-7>
- Smith, A., Martin, D., & Cockings, S. (2016). Spatio-temporal population modelling for enhanced assessment of urban exposure to flood risk. *Applied Spatial Analysis*, 9(2), 145–163. <https://doi.org/10.1007/s12061-014-9110-6>
- Stewart, R., Urban, M., Duchscherer, S., Kaufman, J., Morton, A., Thakur, G., et al. (2016). A Bayesian machine learning model for estimating building occupancy from open source data. *Natural Hazards*, 81(3), 1929–1956. <https://doi.org/10.1007/s11069-016-2164-9>
- Tatem, A. J. (2017). WorldPop, open data for spatial demography. *Scientific Data*, 4, Article 170004. <https://doi.org/10.1038/sdata.2017.4>
- Taubenböck, H., Goseberg, N., Lämmel, G., Setiadi, N., Schlurmann, T., Nagel, K., et al. (2013). Risk reduction at the “last-mile”: An attempt to turn science into action by the example of Padang, Indonesia. *Natural Hazards*, 65(1), 915–945. <https://doi.org/10.1007/s11069-012-0377-0>
- Taubenböck, H., Roth, A., & Dech, S. W. (2007). Linking structural urban characteristics derived from high resolution satellite data to population distribution. In M. Rumor, V. Coors, E. M. Fendel, & S. Zlatanova (Eds.), *Urban and regional data management* (pp. 35–45). London: Taylor & Francis.
- Tenzer, F. (2024). Marktanteile der einzelnen Netzbetreiber an den Mobilfunkanschlüssen in Deutschland von 1998 bis 2023. Edited by Statista. Available online at <https://de.statista.com/statistik/daten/studie/3028/umfrage/marktanteile-der-netzbetreiber-am-mobilfunkmarkt-in-deutschland-seit-1998/> (checked on 5/21/2025).
- Tuccillo, J. V., Moehl, J., Adams, D., Cunningham, A. R., Urban, M., Walters, S., et al. (2025). LandScan HD: A high-resolution gridded ambient population methodology for the world. *Population and Environment*, 47(4). <https://doi.org/10.1007/s11111-025-00514-6>
- U.S. Department of Transportation. (2022). National Household Travel Survey - data. Edited by Federal Highway Administration. Available online at <https://nhts.ornl.gov/>.
- UNDESA. (2019). *World urbanization prospects. The 2018 Revision*. UN Department of Economic and Social Affairs. Available online at <https://www.un-ilibrary.org/content/books/9789210043144>.
- Urban, M., Stewart, R., Basford, S., Palmer, Z., & Kaufman, J. (2023). Estimating building occupancy: A machine learning system for day, night, and episodic events. *Natural Hazards*. <https://doi.org/10.1007/s11069-022-05772-3>
- Wang, Y., & Taylor, J. E. (2018). Coupling sentiment and human mobility in natural disasters: A Twitter-based study of the 2014 South Napa Earthquake. *Natural Hazards*, 92(2), 907–925. <https://doi.org/10.1007/s11069-018-3231-1>
- Wang, Y., Taylor, J. E., & Garvin, M. J. (2020). Measuring resilience of human-spatial systems to disasters: Framework combining spatial-network analysis and Fisher information. *Journal of Management in Engineering*, 36(4), Article 04020019. [https://doi.org/10.1061/\(ASCE\)JME.1943-5479.0000782](https://doi.org/10.1061/(ASCE)JME.1943-5479.0000782)
- Wardle, J., Bhatia, S., Kraemer, M. U. G., Nouvellet, P., & Cori, A. (2023). Gaps in mobility data and implications for modelling epidemic spread: A scoping review and simulation study. *Epidemics*, 42, Article 100666. <https://doi.org/10.1016/j.epidem.2023.100666>
- Wipperman, C. (2016). Mitten im Leben. Wünsche und Lebenswirklichkeiten von Frauen zwischen 30 und 50 Jahren. Kurzfassung. Edited by Federal Ministry for Family Affairs, Senior Citizens, Women and Youth. Available online at <https://www.bmfsfj.de/resource/blob/94352/928434dae7d841aac5d2b0ef137573b/mitten-im-leben-wuensche-und-lebenswirklichkeiten-von-frauen-zwischen-30-und-50-jahren-kurzfassung-data.pdf> (checked on 5/22/2025).
- Xie, P., Li, T., Liu, J., Du, S., Yang, X., & Zhang, J. (2020). Urban flow prediction from spatiotemporal data using machine learning: A survey. *Information Fusion*, 59, 1–12. <https://doi.org/10.1016/j.inffus.2020.01.002>
- Yabe, T., Jones, N. K. W., Rao, P. S. C., Gonzalez, M. C., & Ukkusuri, S. V. (2022). Mobile phone location data for disasters: A review from natural hazards and epidemics. *Computers, Environment and Urban Systems*, 94, Article 101777. <https://doi.org/10.1016/j.compenvurbsys.2022.101777>
- Yabe, T., Zhang, Y., & Ukkusuri, S. V. (2020). Quantifying the economic impact of disasters on businesses using human mobility data: A Bayesian causal inference approach. *EPJ Data Science*, 9(1). <https://doi.org/10.1140/epjds/s13688-020-00255-6>
- Yoongsomporn, T., Varquez, A. C. G., Choi, S., Okumura, M., Hanaoka, S., & Kanda, M. (2025). Spatiotemporal analysis of human mobility in greater Tokyo area using hourly 500 m Mobile spatial statistics from 2019 to 2021. *Urban Science*, 9(2), 50. <https://doi.org/10.3390/urbansci9020050>
- Zhang, F., Li, Z., Li, N., & Fang, D. (2019). Assessment of urban human mobility perturbation under extreme weather events: A case study in Nanjing, China. *Sustainable Cities and Society*, 50, Article 101671. <https://doi.org/10.1016/j.scs.2019.101671>
- Zhang, Y., Zhao, H., & Long, Y. (2025). CMAB: A multi-attribute building dataset of China. *Scientific data*, 12(1), 430. <https://doi.org/10.1038/s41597-025-04730-5>
- Zhao, J., Qu, Q., Zhang, F., Xu, C., & Liu, S. (2017). Spatio-temporal analysis of passenger travel patterns in massive smart card data. *IEEE Transactions on Intelligent Transportation Systems*, 18(11), 3135–3146. <https://doi.org/10.1109/TITS.2017.2679179>
- Zhong, C., Batty, M., Manley, E., Wang, J., Wang, Z., Chen, F., & Schmitt, G. (2016). Variability in regularity: Mining temporal mobility patterns in London, Singapore and Beijing using smart-card data. *PLoS One*, 11(2), Article e0149222. <https://doi.org/10.1371/journal.pone.0149222>
- Zhu, X. X., Chen, S., Zhang, F., Shi, Y., & Wang, Y. (2025). GlobalBuildingAtlas: An open global and complete dataset of building polygons, heights and LoD1 3D models. *Earth System Science Data*, 17(12), 6647–6668. <https://doi.org/10.5194/essd-17-6647-2025>